CANADIAN JOURNAL of
URBAN RESEARCH
REVUE CANADIENNE de RECHERCHE URBAINE

Urban heat island effect in Canada: Insights from five major cities

Yuwei Duan
Department of Earth and Atmospheric Sciences, University of Alberta

Sandeep Agrawal
Department of Earth and Atmospheric Sciences, University of Alberta

Arturo Sanchez-Azofeifa
Department of Earth and Atmospheric Sciences, University of Alberta

Nilusha Welegedara*
Department of Earth and Atmospheric Sciences, University of Alberta

Abstract
Climate change poses a significant global challenge, impacting regions differently. This study quantifies the spatio-temporal patterns of diurnal, monthly, seasonal, and annual average urban heat island (UHI) intensity in Canada, a northern country, using data from five major cities: Toronto, Montreal, Vancouver, Edmonton, and Calgary, based on land surface temperature and land use data. Results indicate that each city exhibits distinct variations in UHI intensity influenced by its location, land use, and climate. In summer, Vancouver has the highest daytime UHI intensity at 7.25°C, while Toronto has the highest nighttime intensity at 4.36°C. In winter, Toronto has the highest daytime UHI intensity at 4.50°C, while Calgary has the highest nighttime intensity at 2.89°C. Edmonton records the lowest winter daytime UHI intensity at -1.29°C, with a nighttime increase reaching 2.86°C, due to the colder surrounding rural areas. Based on the spatial distribution, we found that high UHI intensity areas correlate with dense built-up areas, indicating that increasing urbanization intensifies the UHI effect. We also found that large water bodies have a cooling impact in urban areas during the day. This research can guide sustainable urban planning and policies tailored to local conditions, particularly in cities in Northern countries.

Keywords: Urban Heat Island (UHI), Land Surface Temperature (LST), UHI Spatiotemporal Variation, northern cities

Résumé
Les changements climatiques représentent un défi mondial majeur, qui impacte différemment les régions. Cette étude quantifie les schémas spatiotemporels de l'intensité moyenne diurne, mensuelle, saisonnière et annuelle des îlots de chaleur urbains (ICU) au Canada, un pays nordique, à l'aide de données provenant de cinq grandes villes : Toronto, Montréal, Vancouver, Edmonton et Calgary, basées sur la température de surface terrestre et les données d'utilisation

Canadian Journal of Urban Research, Winter 2024, Volume 33, Issue 2, pages 53–78.

ISSN: 2371-0292

du sol. Les résultats indiquent que chaque ville présente des variations distinctes de l'intensité des ICU, influencées par sa localisation, l'utilisation du sol et le climat. En été, Vancouver présente l'intensité d'ICU la plus élevée le jour, soit 7,25 °C, tandis que Toronto présente l'intensité nocturne la plus élevée, soit 4,36 °C. En hiver, Toronto présente l'intensité d'ICU la plus élevée le jour, soit 4,50 °C, tandis que Calgary présente l'intensité nocturne la plus élevée, soit 2,89 °C. Edmonton enregistre l'intensité d'ICU la plus faible le jour en hiver, soit -1,29 °C, avec une augmentation nocturne atteignant 2,86 °C, en raison des zones rurales environnantes plus froides. D'après la répartition spatiale, nous avons constaté que les zones à forte intensité d'ICU sont corrélées aux zones bâties denses, ce qui indique que l'urbanisation croissante intensifie l'effet ICU. Nous avons également constaté que les grandes étendues d'eau ont un effet rafraîchissant dans les zones urbaines pendant la journée. Ces recherches peuvent orienter la planification urbaine durable et les politiques adaptées aux conditions locales, en particulier dans les villes des pays du Nord.

Mots-clés : Îlot de chaleur urbain (ICU), température de surface terrestre (TST), variation spatiotemporelle de l'ICU, villes du Nord

*Correspondence to: Nilusha P. Y. Welegedara, Department of Earth and Atmospheric Sciences,1-26 Earth Sciences Building, University of Alberta, Edmonton, Canada, T6G 2E3 Email: yalingas@ualberta.ca

Introduction

In recent years, rapid urbanization has led to critical ecological and environmental issues in cities and their surrounding areas (Dalby 2002), contributing significantly to increasing greenhouse gas emissions (Hoornweg et al. 2011; Chien et al. 2022) and accelerating global warming. Large-scale urbanization has also increased land surface temperatures (LST) inside urban areas, leading to the urban heat island (UHI) effect (Li et al. 2017; Parker 2010). Higher temperatures within urban areas raise the frequency of extreme weather events, particularly in the summer months (Kornhuber et al. 2019).

As extreme temperatures become more prevalent worldwide, countries located at high latitudes, such as Canada, are not exempted from this trend (Welegedara et al. 2023). In fact, Canada is experiencing greater warming compared to some other regions, with a warming rate about twice the global average (Wang et al. 2016; Hayes et al. 2022). The Health Canada (2020) report indicates that the rise in outdoor temperatures has led to an increase in heat-related illnesses and deaths in Canada. For instance, in the summer of 2021, 619 people died in British Columbia due to extreme heat (BC Coroners Service 2022). In July 2018, 86 deaths were attributed to heat waves in Quebec (Health Canada 2020). In contrast, a few studies have highlighted the benefits of UHIs. For example, Macintyre et al. (2021) demonstrated that UHIs in winter prevented 266 cold-related deaths in a heavily urbanized UK region in 2009. Lowe (2016) demonstrated that UHIs can prevent four cold-related deaths per million persons in the US. Therefore, understanding the characteristics and variations of UHIs in northern cities is critical to developing effective strategies and urban planning efforts and is worthy of an in-depth study.

The UHI effect, influenced by geographic location, climatic conditions, and land use types, has been widely recognized as a critical urban environmental issue. Recent studies have highlighted the importance of context-specific approaches to UHI modelling and mitigation. Acosta et al. (2023) revealed that universal mitigation strategies of the UHI effect may not produce consistent results across different regions of the world, based on their study of summer UHI in five cities located in three countries with varying climates and urban environments. This suggests that effectively mitigating UHI requires context-specific strategies that account for local conditions, rather than relying on a uniform, global approach. Wang et al. (2025) found that increasing green coverage, especially in high-density urban areas, plays a vital role in mitigating the UHI effect, based on their analysis of nine districts in Chongqing in China. Assaf and Assaad (2023) reviewed 13 engineered UHI mitigation strategies and found that most studies focus on the cooling effect of green roofs (up to 23.9°C), while the social, environmental, and economic benefits of other measures remain underexplored, highlighting the need for broader future assessments.

Our study addresses the gap in the existing research by providing a comprehensive and systematic approach to analyzing UHIs across northern cities. This study aims to analyze and compare the spatial distribution and seasonal variations of UHIs in major Canadian cities in 2021–a warmer year indicative of future trends. According to the National Oceanic and Atmospheric Administration (NOAA) scientists, in 2021, the global surface average temperature

was 1.51°F (0.84°C) higher than the 20th-century average, ranking it as the sixth highest year on record from 1880 to 2021 (NOAA, 2021). This indicates a notable urban heat island (UHI) effect in different cities.

Therefore, focusing on the year 2021 for this study would be conducive to identifying the spatial and temporal distribution patterns of UHI in Canadian cities, which are located at higher latitudes. We selected Toronto, Montreal, Vancouver, Edmonton, and Calgary for the analysis due to their large populations, large urban size, high population density, and high level of urbanization (Newbold 2011). Moreover, these cities have diverse geographical characteristics—Edmonton is positioned significantly northward, characterized as a high latitude city (Welegedara et al. 2023), Calgary is located near the Rocky Mountains, Vancouver is close to the Pacific Ocean, Montreal is an island located in the Saint Lawrence River and Toronto is adjacent to Lake Ontario. Studying these five cities could provide valuable insights urban ecosystems and promoting sustainable urban development. Identifying suitable mitigation measures is particularly challenging for large northern countries such as Canada due to the complex temporal and spatial variations of weather variables. This study explores variations in UHI effects across major cities in primarily considering two opposite extreme temperature periods and geographical factors such as proximity to large water bodies or mountains–an area that has not been explored in the existing literature. This focus on both temporal and spatial factors highlights the novelty of the study. Further, identifying the similarities and differences in UHI effects among the northern cities can provide valuable insights for planners, helping them develop unified plans and draw inspiration from one another, particularly when implementing UHI mitigation measures and strategies.

Literature review

The UHI refers to the phenomenon of higher temperatures in urban areas than in the surrounding rural areas (Maimaitiyiming et al. 2014). This phenomenon mainly results from the absorption, storage and re-emitting of solar radiation by the urban structures (Rizwan et al. 2008). The concept of UHI was first observed by Luke Howard in 1833, who noticed that urban areas tend to have higher temperatures than their surrounding regions (Oke 1982). Subsequently, Manley (1958) introduced the term "urban heat island" in 1958. Initially, the researchers calculated the UHI intensity using air temperatures from observation stations (Oke 1973). In recent years, satellite-obtained surface temperature data, such as Landsat and MODIS data, have become increasingly prevalent in the study of UHI (Zhou et al. 2014; Li and Zhou 2019).

The UHI is generally calculated by subtracting the rural temperature from the urban temperature (Hardin et al. 2018). UHI research can be classified into two types based on the different methods of obtaining temperature data: UHI based on air temperature and UHI based on land surface temperature (Imhoff et al. 2010; Zhou et al. 2014). Specifically, when the land surface temperature is used to calculate UHI intensity, it is referred to as surface urban heat island intensity (SUHII) (Peng et al. 2012). The UHI based on air temperature is determined using observed data from ground-based meteorological stations. However, this UHI value is sensitive to various factors such as the selection of indicators, environmental influences, and experimental conditions (Schwarz et al. 2012). Moreover, Stewart (2011) suggested that the UHI research based on meteorological data often lacks comparability due to uncontrollable factors such as weather, topography, or time. In contrast, SUHII is less affected by these factors and offers more comparable results.

According to existing research, UHI exhibits diurnal, seasonal, and regional variations. By analyzing SUHI in 419 large cities around the world, Peng et al. (2012) found that SUHII was higher during the day than at night, but no correlation between daytime and nighttime SUHII. Santamouris (2015) found that there are obvious seasonal variations in the UHI effect in Asia and Australia. Zhao et al. (2014) studied 65 major cities in North America and found that local climate has a strong influence on UHI. Additionally, Wienert and Kuttler (2005) found that the higher the latitude, the higher the UHI. By analyzing the UHI in 28 cities situated in northern West Siberia at 60° north latitude, Miles and Esau (2017) discovered that the average UHI is higher in winter than in summer, and they also noted a strong correlation between the UHI of high-latitude cities and population density and surrounding temperature. Welegedara et al. (2023) found that, in Edmonton, while UHI occurred in winter and spring, summers experienced higher UHI.

In addition, different types of land cover have a significant impact on UHI development. Rinner and Hussain (2011)'s study conducted in Toronto demonstrated that the average temperature is significantly higher in commercial and industrial areas, and lower in non-built-up areas such as parks and water bodies. The size of the city also affects the UHI. Gaur et al. (2018) analyzed surface temperature data from 20 Canadian cities between 2002 and 2010

and used predictive models to forecast future trends. They found that by 2100, more than half of the 16 Canadian cities previously affected by UHI will experience an increase in UHI intensity, with larger cities experiencing a more significant rise. Therefore, it is critical to study the current state of UHI in major Canadian cities and to develop and implement effective strategies to mitigate UHI intensity.

MODIS and Landsat satellite imagery are frequently used to calculate UHI, and each type of imagery has its own advantages and limitations. Landsat 8 data has a better spatial resolution (resampled to 30 m), enabling a clearer identification of hotspots (Sidiqui et al. 2016). On the other hand, MODIS data offers a higher temporal coverage (twice daily), providing data for both daytime LST (form MYD11A1) and nighttime LST (form MOD11A1). The high temporal resolution of MODIS has led many researchers to consider MODIS data as a better choice for studying UHI in a larger region (Tomlinson et al. 2012). Therefore, we used MODIS for this analysis, specifically to compare cities across the country using different time variables, including diurnal and seasonal variations.

Most studies on UHI focus on mid- and low-latitude regions, while research on UHI in northern areas remains limited (Drebs et al. 2023). Miles et al. (2020) conducted a study on urban heat islands (UHI) in 57 cities across the high-latitude region of northern Fennoscandia, which includes the countries Finland, Norway, and Sweden. However, in Canada, another northern country, existing research has primarily focused on individual cities. There is still a lack of studies that analyze and compare UHI across multiple cities with varying geographic and climatic conditions. This research seeks to address this gap.

Study area, data and methodology

Study area

Canada is the second largest country in the world in terms of its land mass, spanning approximately 4,634 kilometers from north to south and about 5,514 kilometers from east to west (Statistics Canada n.d.). However, the population of Canada is relatively small, with approximately 40 million people (Statistics Canada 2022) and is mainly concentrated in the southern regions closer to the Canada-USA border. In this study, we selected five major Canadian cities, including Toronto, Montreal, Vancouver, Edmonton and Calgary, as case studies. These cities were selected because of their larger areas and populations, diverse geographical features, and their distinct locations within the country. Figure 1 shows the geographical locations of five cities across Canada and the census tract maps for each city. Edmonton and Calgary are prairie cities. Vancouver is located on the west coast of Canada and is a coastal city. Montreal and Toronto are situated in the center area of the country next to the St. Lawrence River and the Great Lakes, respectively.

Table 1 shows the population, area, population density, location, and elevation of each city. As shown in Figure 1 and Table 1, Edmonton is the northernmost and Toronto is the southernmost among the five cities. Toronto has the largest population, while Vancouver has the smallest. However, Vancouver has the highest population density, and Edmonton has the lowest. Calgary is situated at the highest elevation due to its proximity to the mountain region, in contrast with Vancouver, which is at the lowest elevation.

Data

Land cover/land use data. In this study, we used publically available land use land cover (LULC) data from the European Space Agency's (ESA) Sentinel-2 imagery, acquired in 2021, with a spatial resolution of 10m (https://www.arcgis.com/apps/instant/media/index.html?appid=fc92d38533d440078f17678ebc20e8e2). In addition, referring to the land classification methodology described by Schneider et al. (2009), we classified the original data into eight land types that are built-up, croplands, trees, shrubs and grasslands, flooded vegetation, bare grounds, surface water bodies, as well as snow and ice.

Land surface temperature data. MODIS land surface temperature (LST) data were derived from Terra and Aqua satellite images (Zhu et al., 2013). In this study, we used the MYD11A1 data from the Aqua satellite to obtain daytime LSTs, and MOD11A1 data from the Terra satellite to obtain nighttime LSTs. The spatial resolution of MODIS LST data is 1km. The calculation formula of surface temperature is as follows:

Figure 1
Study area

Table 1
Basic information of each city in 2021

City	Population	Area (km^2)	Population density (per km^2)	Location ($°N$)	Longitude ($°W$)	Elevation (m)
Edmonton	1,010,899	765.61	1320.4	53	113	670
Calgary	1,306,784	820.62	1592.4	51	114	1,060
Vancouver	662,248	115.18	5,749.9	49	123	34
Toronto	2,794,356	631.10	4427.8	43	79	76
Montreal	1,762,949	364.74	4833.4	45	73	112

Data source: Statistics Canada Census Profile; 2021 Census of Population

$$T = (DN \times 0.02) - 273.15 \quad \text{(Equation 1)}$$

Where, *DN* is the brightness value of the pixel, and T is the surface temperature *(°C)* (Wan 2014). Using Google Earth Engine (GEE) code, we can calculate and directly download the monthly average land surface temperature (LST) for daytime and nighttime in batches, with quality control applied, for each city. This approach significantly enhances work efficiency. Therefore, in this paper, we use GEE codes to directly obtain the monthly average LST data for both daytime and nighttime from MYD11A1 and MOD11A1 for each city.

Methodology

Defining urban and rural areas. In this study, we described the urban boundary of each city based on the built-up surfaces in residential, industrial, transportation and other construction areas within the city. The built-up area refers to the non-agricultural construction area that developed through construction activities in the administrative area (Zhang et al. 2018). We then demarcated the rural area of each city by creating buffer zones that extended outward from the built-up boundaries. The buffer distance varies depending on the size of the city, and the total buffer area was approximately twice the size of the built-up area to accurately identify the surrounding rural areas (Zhou et al. 2015; Welegedara et al. 2023). The buffer zone distances for Vancouver, Edmonton, Toronto, Montreal, and Calgary are 10, 5, 15, 10, and 5 km from their respective city boundaries. However, due to urban development and expansion, built-up areas, including buildings and roads, exist within the buffer zones or rural areas, which may influence the UHI intensity values. Therefore, we removed these built-up areas from the buffer zones. Figure 2 illustrates the schematic representation of urban and rural areas, as well as the different land use cover types in Edmonton as an example.

Calculation of urban heat island intensity. We derived the UHI intensities in each city using MODIS LST data as indicated in Equation 2 to compare UHI intensities in different cities.

$$SUHII = T_u - T_r \qquad \text{(Equation 2)}$$

Where *SUHII* is the intensity of the surface urban heat island, T_u is the urban surface temperature, and T_r is the rural surface temperature. Positive UHI intensity indicates that the urban area is experiencing higher temperature than that of the rural areas. In contrast, negative intensity indicates an urban heat sink or cooler urban areas than rural (Clinton and Gong 2013).

In order to analyze the similarities and differences of UHI intensity in the five cities, we calculated the monthly and annual averages, and seasonal day and night averages for each considered city. We considered the four seasons as follows: June, July and August as summer; September, October and November as autumn/fall; December, January and February as winter; and March, April and May as spring.

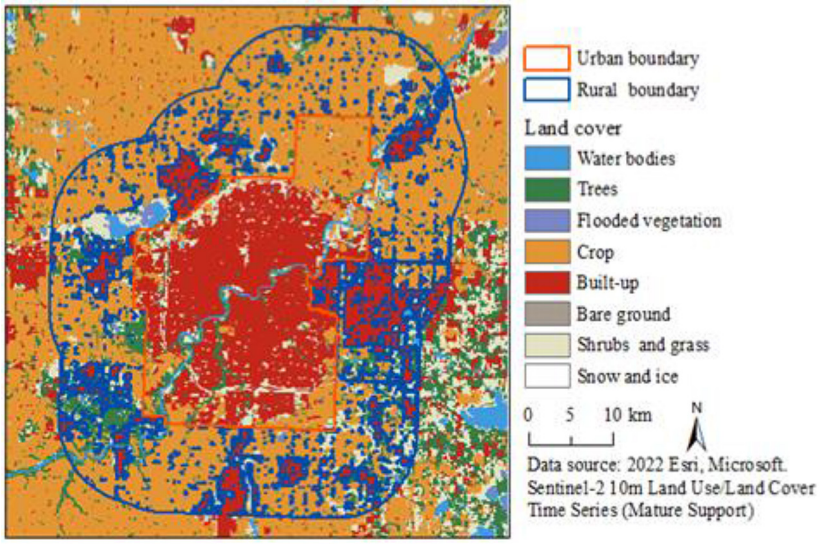

Figure 2
Schematic diagram of urban and rural areas, using Edmonton as an example

Hotspot analysis. In this study, we used the Getis-Ord Gi* to conduct the hotspot analysis which can statistically identify spatial clusters of high (hotspots) and low (cold spot) values. The calculation formula of Getis is as follows:

$$Getis = \frac{\sum_{j=1}^{n} W_{i,j}\, x_j - \bar{x} \sum_{j=1}^{n} W_{i,j}}{S\sqrt{\frac{\left[n\sum_{j=1}^{n} W^2{}_{i,j} - \left(\sum_{j=1}^{n} W_{i,j}\right)^2\right]}{n-1}}} \quad \text{(Equation 3)}$$

$$\underline{x} = \frac{\sum_{j=1}^{n} x_j}{n} \quad \text{(Equation 4)}$$

$$S = \sqrt{\frac{\sum_{j=1}^{n} x^2 j}{n} - (\bar{x})^2} \quad \text{(Equation 5)}$$

where x_j represents the attribute of element j; $W_{i,j}$ represents the spatial weight between element i and j; n represents the total number of samples (Esri n.d.).

Results

Spatial and temporal distribution of annual average daytime and nighttime LST

Figure 3 illustrates the distribution of the annual average day and night LST at the census tract level for each city, based on observations from the MODIS satellite in 2021. The LST fluctuates with the surface energy balance, which refers to the balance between the energy the Earth's surface receives and the energy it loses (Clinton and Gong 2013) and is controlled by surface radiation and thermodynamic properties, including surface humidity, thermal conductivity and surface emissivity, surface radiation input from the solar energy and atmosphere, as well as the influence of the near-surface atmosphere and the turbulent effect of ground gasses (Voogt and Oke 2003). As shown in Figure 3, the spatial distribution of the LST varies from city to city. Calgary and Edmonton exhibit similar patterns in daytime and nighttime LST distribution, with temperatures being higher in the city centre during both day and

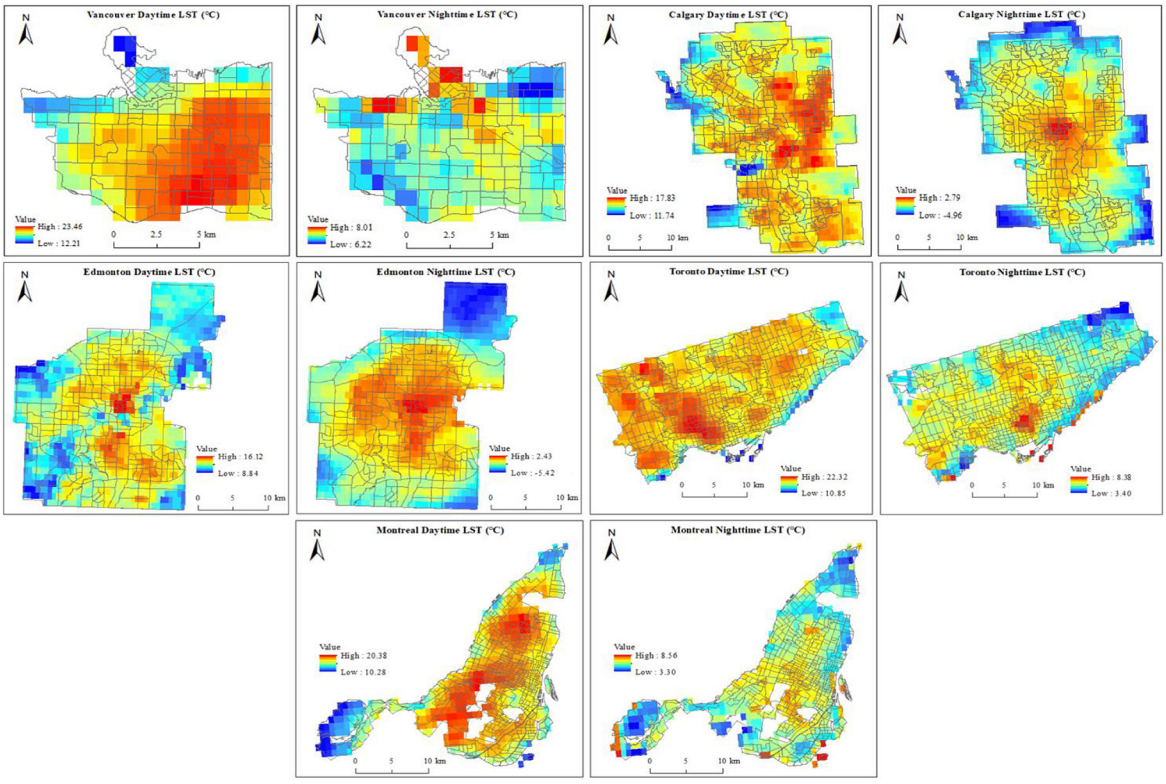

Figure 3
Annual average day and night LST distribution maps

Table 2
Annual average day and night LST (°C) in 2021 for each city

City	Vancouver	Edmonton	Calgary	Toronto	Montreal
Daytime LST	20.17	12.94	15.81	19.54	17.00
Nighttime LST	7.15	-1.01	-1.05	5.67	5.57

night, dispersing outward. In Edmonton, the centres of high temperatures, particularly downtown, surrounding areas and the industrial areas, show a similar pattern during both day and night. During the day, the temperatures near the river valley area are lower, but at night, they are relatively higher. In Calgary, the centres of high temperatures differ slightly between day and night, but the LST distribution patterns are similar throughout. Nevertheless, in Vancouver, Toronto, and Montreal, the daytime and nighttime LST patterns are opposite. In these three cities, especially in Vancouver, the high temperature areas during the day are concentrated in the inland areas of the city centre, while at night; the high temperature areas are concentrated near large water bodies, such as oceans, lakes, and rivers. This is mainly because water has a high specific heat capacity and strong thermal inertia. Thus, water bodies absorb heat during the day and release it slowly at night, resulting higher nighttime LSTs .

As shown in Table 2, the annual average of daytime LST is higher than nighttime LST in all five cities. Calgary showed the largest temperature difference between day and night (16.86˚C), followed by Edmonton (13.95˚C), Toronto (13.87˚C), Vancouver (13.02˚C) and Montreal (11.43˚C). Vancouver is the warmest city during both the day and night, having the highest average LST followed by Toronto and Montreal. Edmonton showed the lowest annual average LST during the daytime, whereas Calgary showed the lowest value at nighttime.

The difference in temperature between the city with the highest daytime temperature (Vancouver) and the lowest daytime temperature (Edmonton) is 7.23˚C, while the difference in temperature between the city with the highest nighttime temperature (Vancouver) and the city with the lowest nighttime temperature (Calgary) is 8.20˚C.

Variations of land use and land covers in the major cities and the effect on LST

To understand the impact of different land use types on LST, we first analyzed LULC types of the five cities. Figure 4 shows the distribution of LULC types in five cities. These LULC data were obtained using ESA Sentinel-2 imagery (Esri) 2022). As shown in Figure 4, built-up areas of Vancouver, Toronto and Montreal cover the majority of the urban area, while the cities of Calgary and Edmonton are surrounded by large agricultural areas around the city in addition to built-up areas. In addition, it can be seen that Vancouver, Toronto and Montreal have more tree cover and fewer shrub and grasslands within their cities, while Calgary and Edmonton have more shrub and grass cover than tree cover. Vancouver and Montreal have large, dense tree covers, while the other three cities have less tree covers.

In this study, we calculated the average day and night LST for different land cover types (Table 3). To account for the resolution differences between the LST data and the land use and land cover data, we first vectorized the land cover map. This allowed us to calculate the LST values for each land parcel type individually, followed by the computation of average value and standard deviation. In general, the higher daytime LST was observed in the built-up area, and the lower daytime LST was observed in the vegetated areas. However, in Vancouver, the highest daytime LST was recorded in the grass areas. It is important to note that the standard deviation of the daytime LST in the grass areas is 2.52, indicating significant data variation, i.e. the difference of the daytime LST between different grass areas is quite large. In Edmonton, Calgary and Toronto, daytime LST is highest in built-up areas, while in Montreal, daytime LST is highest in bare ground, followed by built-up areas. Areas covered by trees have the lowest daytime LST in Calgary. However, in Edmonton, Toronto and Montreal, the crop areas showed the lowest daytime LST. In Vancouver, bare grounds near the ocean have the lowest daytime LST and treed areas have relatively lower daytime LST. However, the standard deviation of the daytime LST in the treed areas in Vancouver is 5.13, demonstrating a significant variation in the data, i.e., the daytime LST in the treed area fluctuated greatly.

During the night, built-up areas have the highest LST and the crop areas show the lowest LST in Edmonton and Calgary similar to what was observed during the daytime. In Vancouver, the highest LST at night is in the treed area, followed by the bare ground, and the lowest LST at night is in the crop area, which is different from the daytime situation. These results indicate that the proximity to large water bodies significantly influences the LST and that the

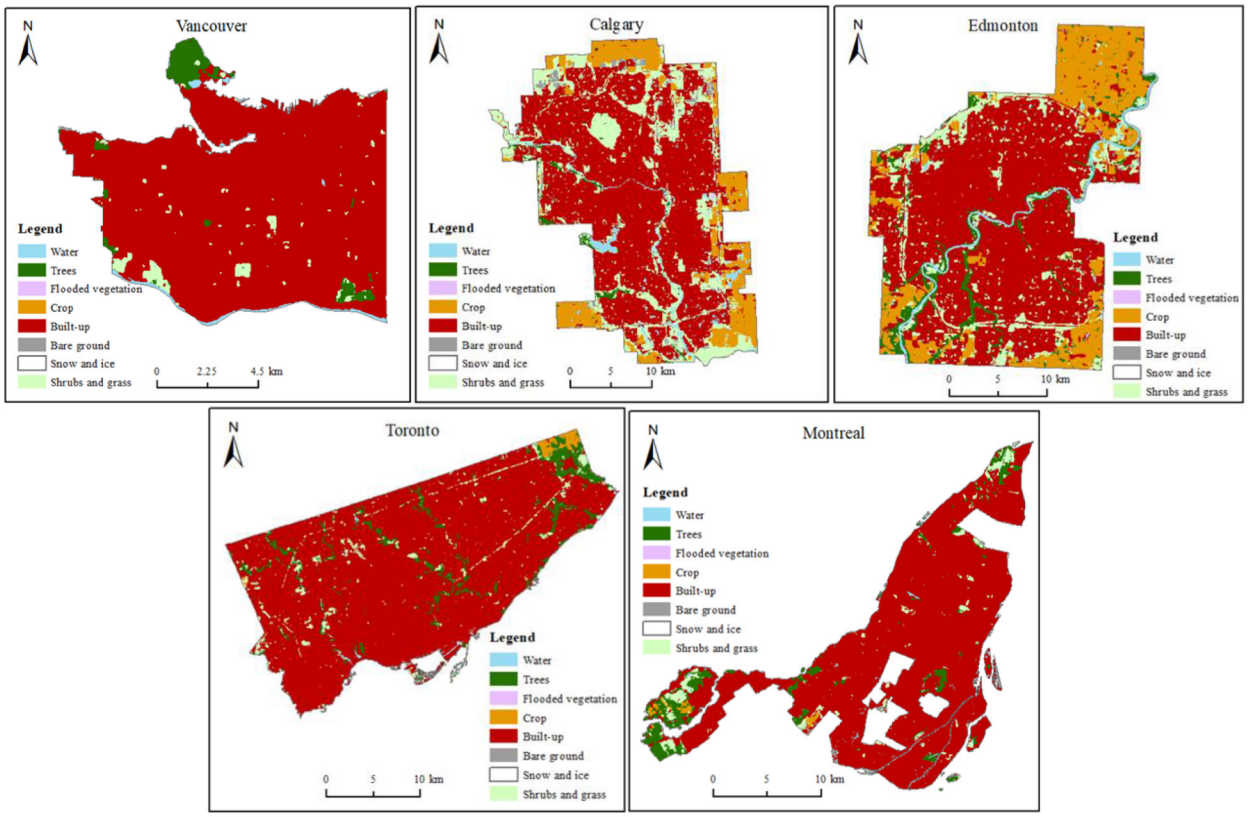

Figure 4
Land use and land cover maps of major cities

UHI intensity is related to the spatial distribution of different land uses. The land type with the highest nighttime LST in Montreal remains the same as during the daytime, and remains bare ground, while the lowest nighttime LST in Montreal is found in grass areas. In Toronto, it is also the bare ground that has the highest nighttime LST, yet it is the crop areas that have the lowest nighttime LST.

Additionally, Table 3 shows that trees are more effective in cooling urban areas during daytime than shrubs or grass, due to their ability to provide shade and facilitate evaporative cooling. City-wise, Vancouver's built-up areas exhibit the highest daytime LST, followed by Toronto, while Edmonton's built-up areas show the lowest daytime LST. Vancouver's built-up areas continue to have the highest LST at night, followed by Toronto. However, different from the daytime, Calgary's built-up area has the lowest LST at night.

Annual average day and night urban heat island characteristics

Figure 5 illustrates the spatial distribution characteristics of the annual average UHI intensity for the five cities during daytime and nighttime. As shown in the daytime UHI intensity distribution, Vancouver, Toronto, and Montreal have higher UHI intensity levels than Calgary and Edmonton. The UHI intensity is above 9.9°C in southeast Vancouver and mostly above 6.5°C in the central regions of Montreal and Toronto. The central area of northern Edmonton has a UHI intensity of over 5.6°C. Nevertheless, in the vast majority of Calgary, the UHI intensity does not exceed 3.9°C. In addition, each city shows a negative UHI intensity in some areas (Figure 5), which indicates that the urban heat sink occurs in some areas of each city (Clinton and Gong 2013). For example, the UHI intensity is negative in the Edmonton River Valley region and west of Calgary due to the influence of water bodies and surrounding tree cover. Moreover, in certain areas near the large water bodies, i.e. ocean and river, of Vancouver and Montreal, the UHI intensity is even below -5.4°C. The distribution of nighttime UHI intensity is the opposite of that during the day, Calgary and Edmonton have higher UHI intensity than Vancouver, Toronto and Montreal. The nighttime UHI intensity in the central parts of Edmonton and Calgary is above 5.2°C, while the nighttime UHI intensity in most

Table 3
Annual average day and night LST for different land cover types

Daytime							
City		Built-up	Crop	Trees	Grasses	Bare ground	Water body
Vancouver	Mean (℃)	20.26	17.90	15.62	20.81	15.32	17.48
	Std dev.	2.33	0.00	5.13	2.52	0.37	0.00
Edmonton	Mean (℃)	13.36	12.11	12.23	12.90	13.33	12.32
	Std dev.	1.00	0.80	1.08	1.15	1.29	1.26
Calgary	Mean (℃)	16.04	15.26	14.69	15.48	14.92	15.30
	Std dev.	0.88	0.96	1.23	1.07	1.02	1.29
Toronto	Mean (℃)	19.70	16.20	18.22	19.17	17.85	17.39
	Std dev.	1.38	0.35	2.07	1.90	0.00	2.59
Montreal	Mean (℃)	17.48	13.01	13.35	14.89	18.93	15.02
	Std dev.	1.93	3.31	2.54	2.91	1.03	2.95
Nighttime							
City		Built-up	Crop	Trees	Grasses	Bare ground	Water body
Vancouver	Mean (℃)	7.14	6.86	7.57	7.07	7.40	7.03
	Std dev.	0.33	0.00	0.41	0.22	0.58	0.00
Edmonton	Mean (℃)	-0.13	-3.31	-1.36	-1.18	-1.41	-0.52
	Std dev.	1.26	1.24	1.65	1.26	0.94	1.53
Calgary	Mean (℃)	-0.52	-3.21	-1.65	-1.59	-1.74	-1.25
	Std dev.	1.06	1.01	1.39	1.15	0.70	1.22
Toronto	Mean (℃)	5.70	3.84	5.51	5.56	6.71	6.12
	Std dev.	0.61	0.35	0.76	0.77	0.00	0.85
Montreal	Mean (℃)	5.64	4.82	5.13	4.76	6.14	5.72
	Std dev.	0.69	1.40	1.37	0.73	1.12	0.97

parts of Vancouver and Montreal is below 2.8°C.

Figure 6 shows the Hot spots map of daytime and nighttime UHI intensity for each city. As shown in Figure 6, the daytime and nighttime UHI in these five cities demonstrate spatial clustering patterns with distinct hotspots and cold spots, indicating the presence of significant spatial autocorrelation in the UHI phenomenon. It can be seen that the daytime and nighttime hotspot distributions differ significantly among the five cities, while the cold spots are generally similar.

Figure 7 shows the distribution and differences in UHI effects during the daytime and nighttime across five cities. However, there are significant variations between the cities. The annual average daytime UHI intensities are higher than the annual average nighttime UHI intensities in Vancouver, Toronto, and Montreal, with the exception

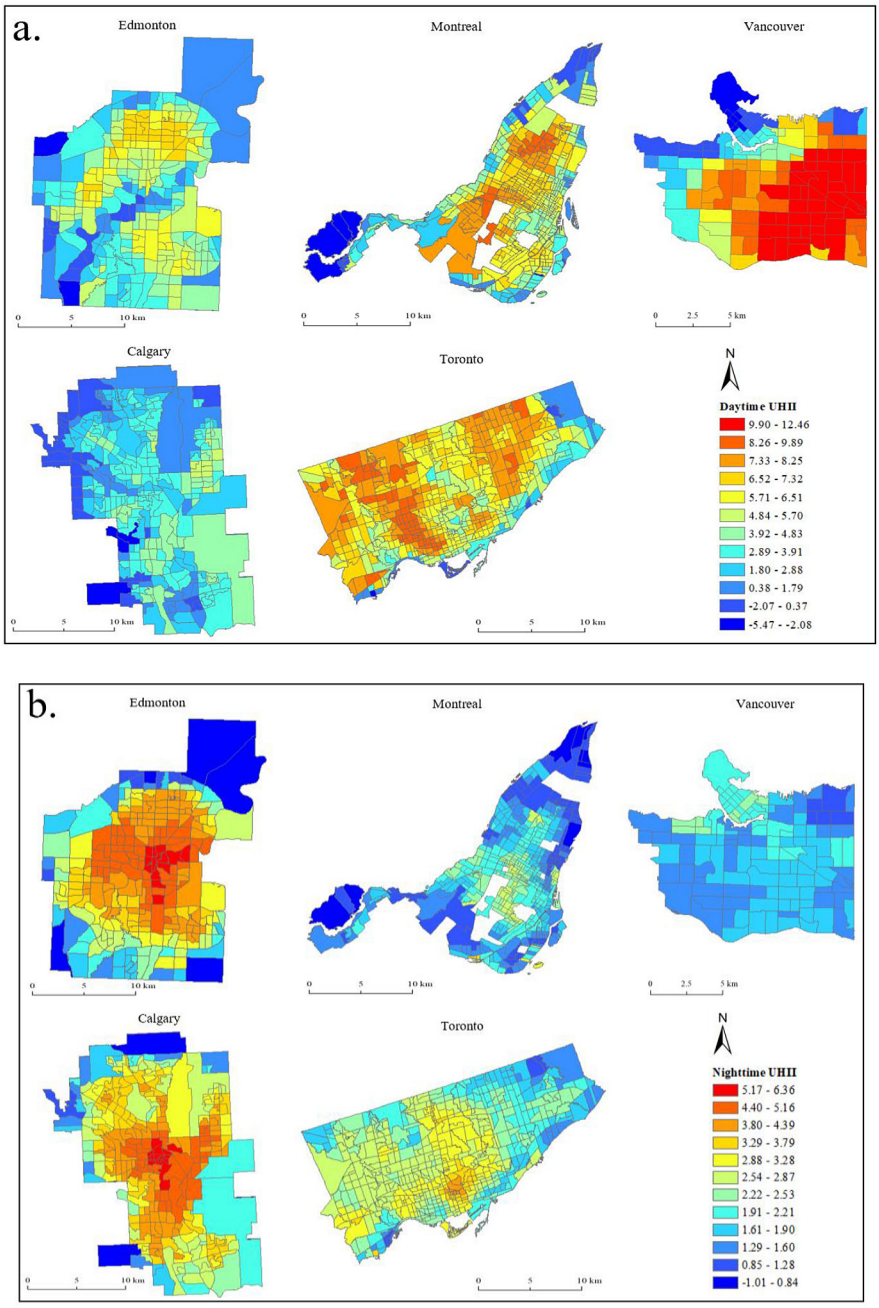

Figure 5
Annual average (a) day and (b) night UHI distribution maps

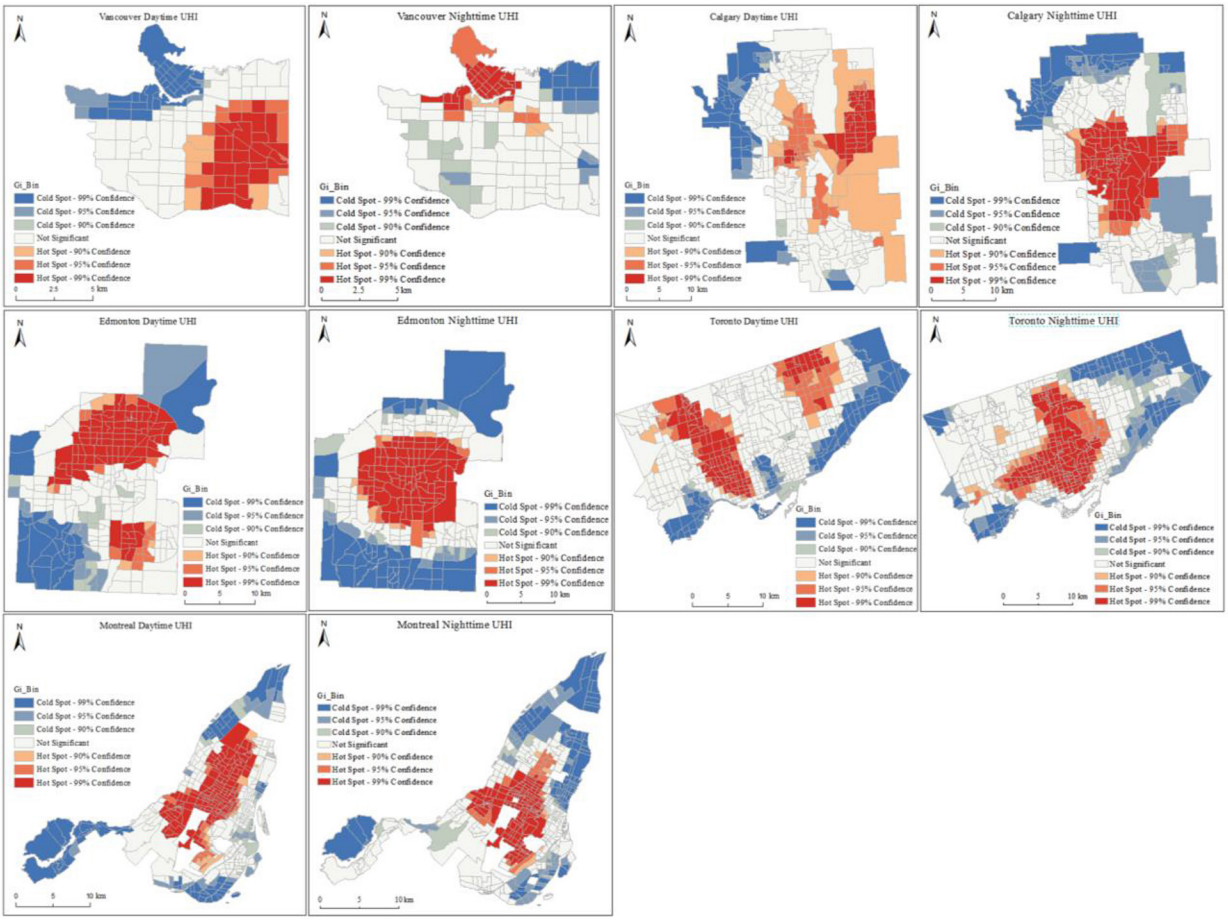

Figure 6 (top)
Daytime and Nighttime UHII Hot spots map

Figure 7 (Bottom)
Box Plot of Daytime and Nighttime UHI Intensity Across Five Cities. Statistical significance between daytime and nighttime is indicated by *p < 0.05, **p < 0.01, ***p < 0.001

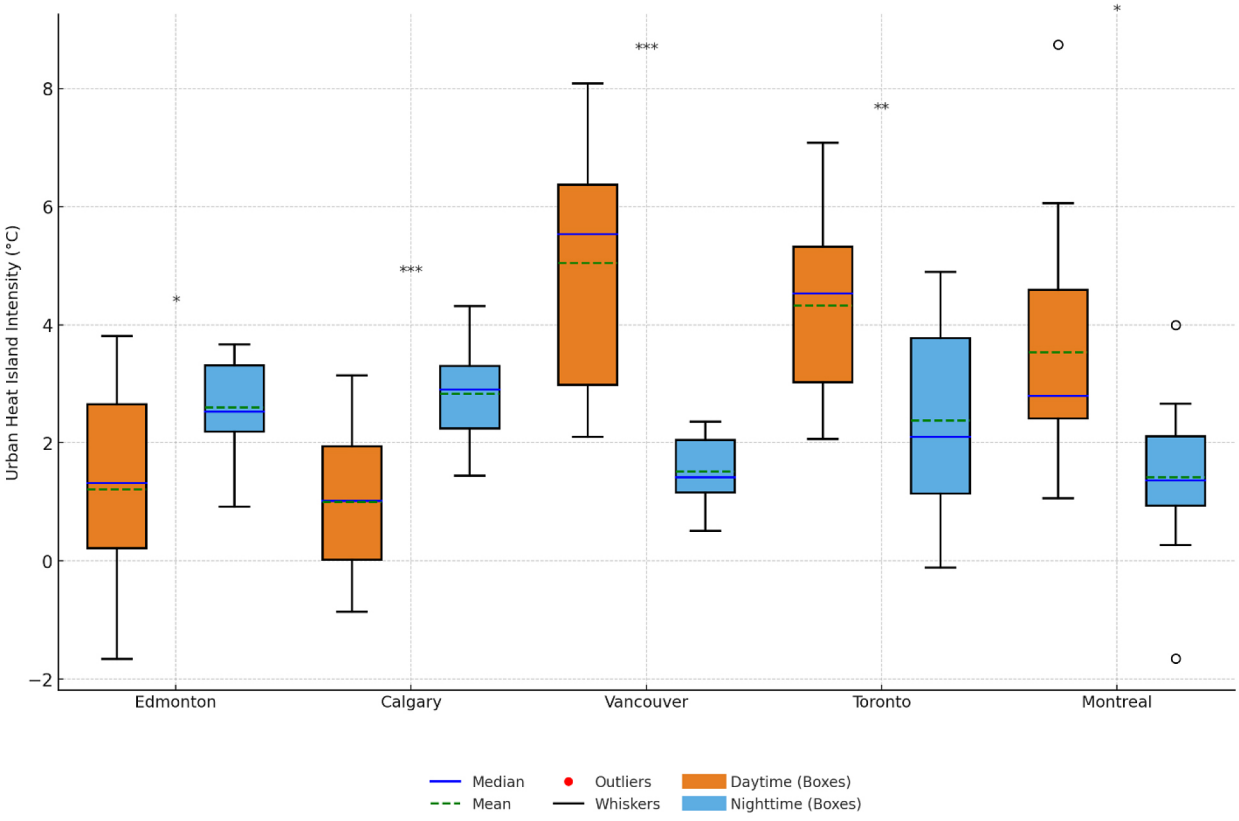

of Calgary and Edmonton, where the nighttime UHI intensities are higher than the daytime UHI intensities (Figure 7). During the day, Vancouver has the highest average annual UHI intensity at 5.04°C, followed by Toronto at 4.32°C, and Calgary has the lowest at only 1.00°C. At night, Calgary has the highest average annual UHI intensity at 2.83°C, followed by Edmonton at 2.60°C. Montreal has the lowest at 1.42°C, while Vancouver is slightly higher than Montreal at 1.52°C. The p-values indicate significant differences in UHI between the daytime and nighttime in the considered cities (Figure 7). Among them, Vancouver, Calgary and Toronto exhibit both statistically and practically significant UHI differences between daytime and nighttime. In contrast, Edmonton and Montreal show statistically significant differences, but the actual magnitude of the differences is relatively small. Additionally, Vancouver exhibits greater variability in daytime UHI, with a wider range that may reflect seasonal differences, but becomes more consistent at night. Toronto's daytime UHI is high but consistent, with less variation across seasons. Montreal's UHI values are stable for both daytime and nighttime, showing less fluctuation throughout the year. Extreme weather conditions might cause outliers in Montreal. Edmonton and Calgary show a consistent nighttime UHI distribution, indicating smaller fluctuations throughout the year, potentially due to less pronounced seasonal climate variations.

Monthly variation of average day and night urban heat islands

In Figures 8 and 9, the shifting trends of monthly average daytime and nighttime LST and UHI are presented. Daytime LST in the five cities is approximately the same from April through September, with Vancouver experiencing higher temperatures from January through March and Toronto experiencing higher temperatures from October through December (Figure 8). However, Vancouver's daytime UHI intensity values are only higher than other cities from April to July, while Calgary's daytime UHI intensity values consistently maintain the lowest all year, except for January and December when it is the lowest in Edmonton.

In addition, Montreal has a very large increase in daytime UHI intensity in March, and a small increase in Edmonton and Calgary. This phenomenon can be attributed to the extremely cold winters in all three cities, with

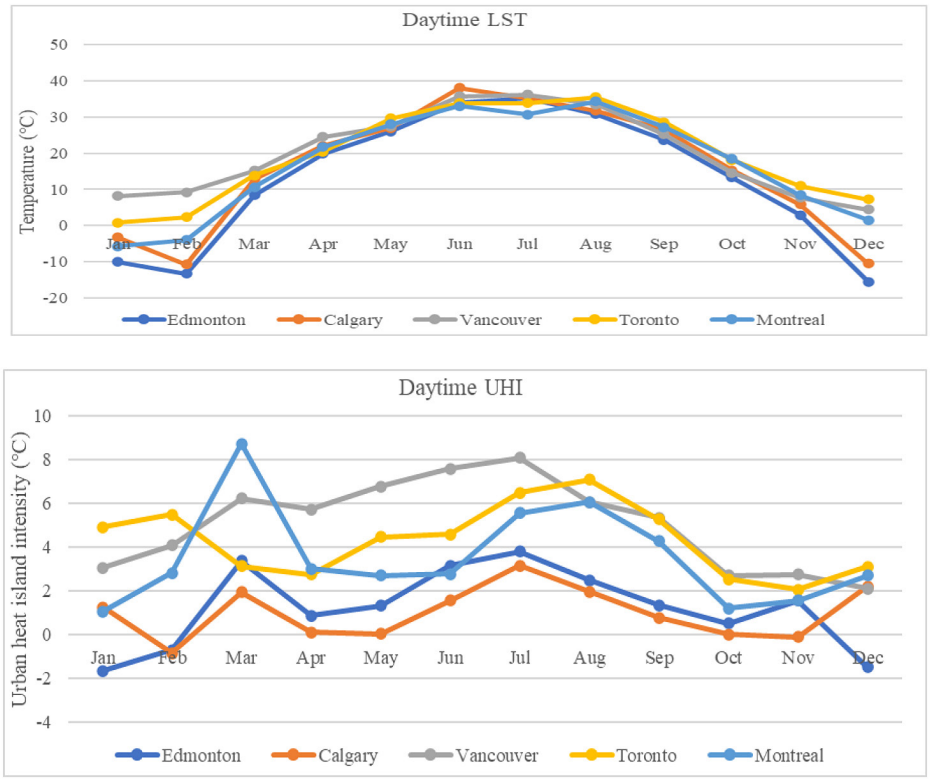

Figure 8
Monthly average daytime LST and UHI intensity

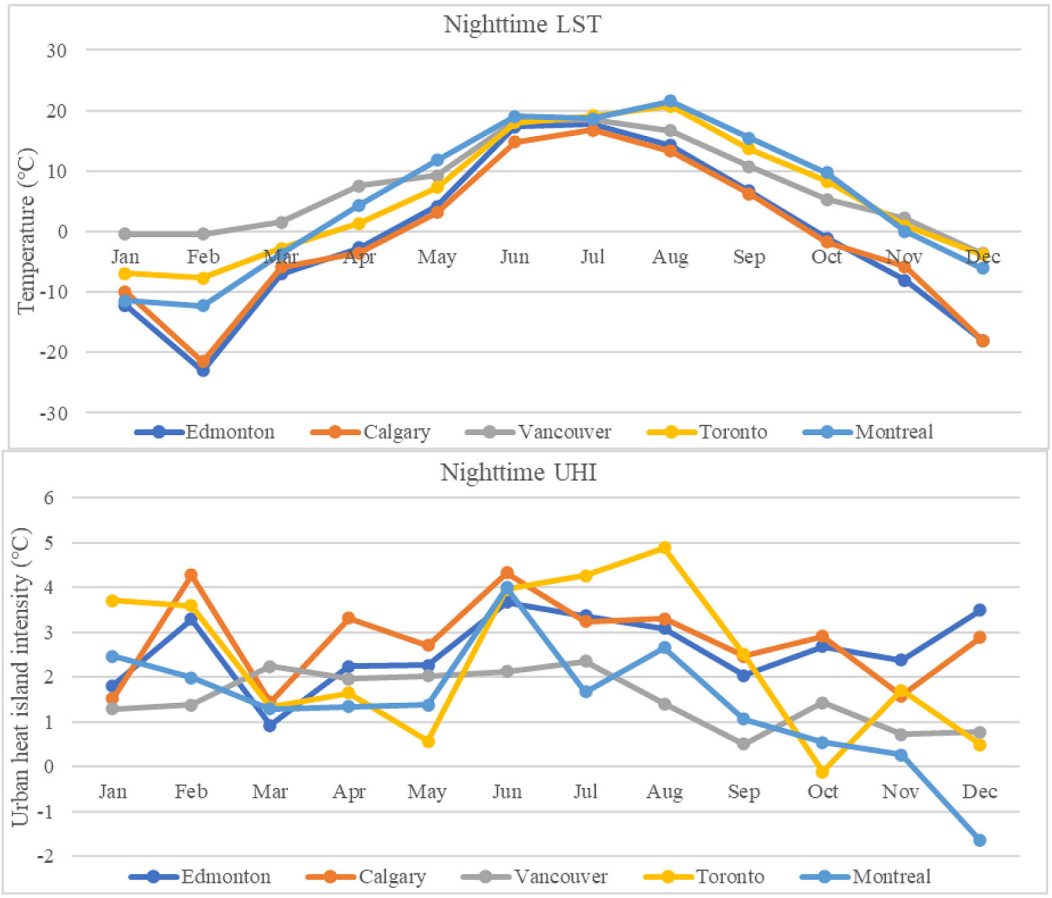

Figure 9
Monthly average nighttime LST and UHI intensity

daytime LST falling below -10°C, and nighttime LST even below -20°C in Edmonton and Calgary in February. As temperatures warmed up in March, the snow in the cities was cleared, while the rural areas still retained snow and ice. This created a substantial temperature difference between the urban areas and the rural areas, contributing to the significant increase in daytime UHI intensity in Montreal and a relatively smaller rise in Edmonton and Calgary.

In comparison to daytime, the fluctuations in both LST and UHI intensity during the nighttime are more pronounced in all five cities, with larger ups and downs. The trends in nighttime LST vary across the five cities, with only Calgary and Edmonton showing similar trends, but all of the nighttime UHI intensity trends are quite different (Figure 9). Among them, Toronto has the most fluctuating trend in the nighttime UHI intensity variation, while Vancouver has the smoothest UHI intensity variation trend. The nighttime UHI intensity in Toronto dropped significantly in October because rural areas around Toronto were warmer than urban areas during that time, a phenomenon known as the urban heat sink.

Given that the UHI intensity in Vancouver and Toronto is significantly higher during the daytime and nighttime compared to other cities, possibly due to the influence of nearby large water bodies (i.e., the North Pacific Ocean and Lake Ontario, respectively), we conducted an analysis of the variations in the annual average LST for both urban and rural areas at different distances from these large water bodies in both cities. Additionally, we also examined the differences in LST between the urban and rural regions at the same distance from the water bodies. To achieve this, we created buffer zones at one-kilometer intervals around the water bodies. This allowed us to obtain urban and rural area bands at varying distances from the water bodies. We then calculated the LST for each area band and determined the temperature differences between the urban and rural bands located at the same distance from the water bodies.

The results indicate that in Vancouver, during the daytime, the closer the distance to the water bodies, the lower the LST in the urban area and the higher the LST in the rural area (Figure 10). Therefore, the daytime LST

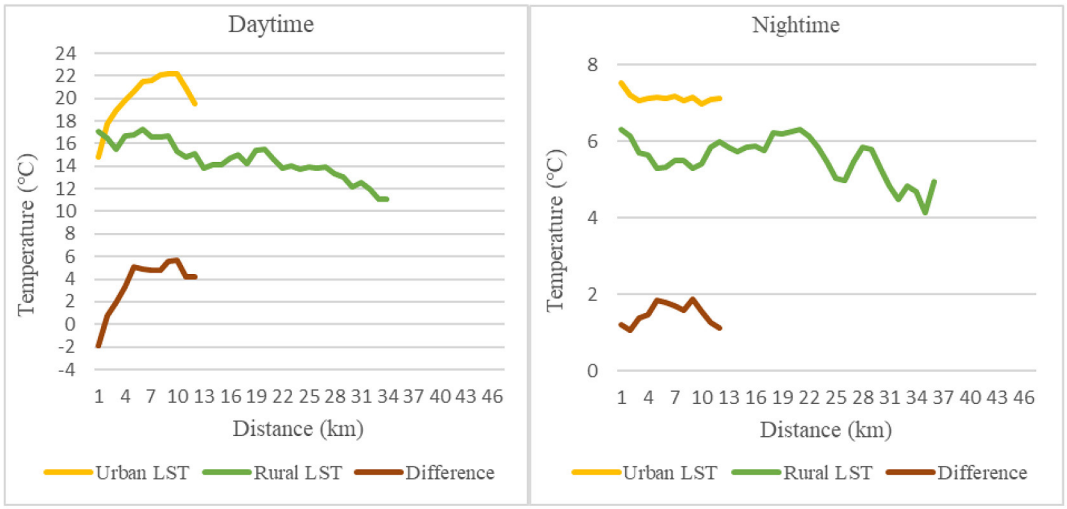

Figure 10
Urban and rural LST at different distances from water bodies in Vancouver

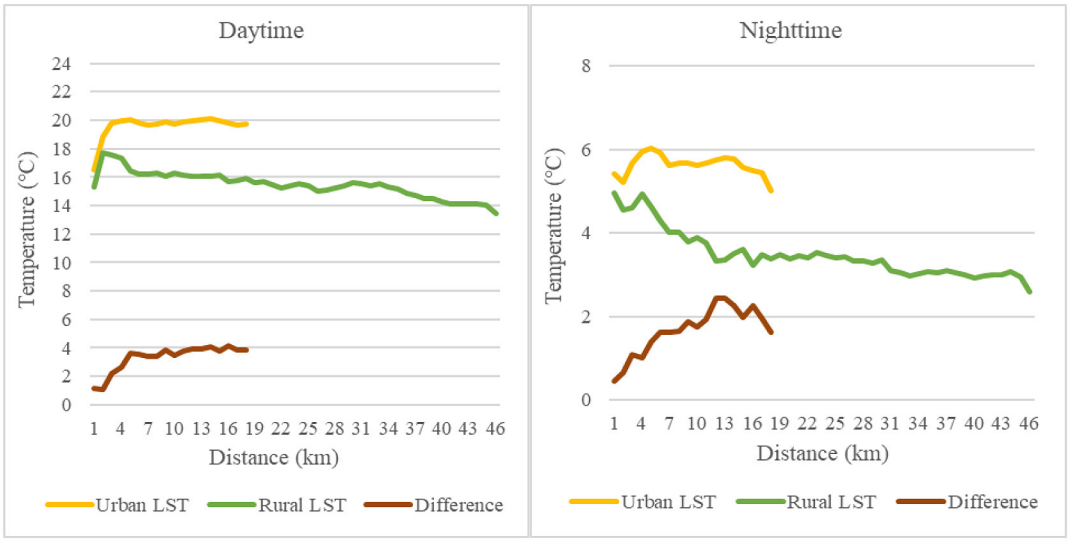

Figure 11
Urban and rural LST at different distances from water bodies in Toronto

difference between the urban and rural areas at the same distance from the water bodies increases with the distance, indicating that the North Pacific Ocean has a significant influence on reducing the daytime UHI intensity in Vancouver, particularly in areas closer to the Ocean. On the other hand, the variation trend of the nighttime LST in urban areas is not very different from that in rural areas, so the variation of the LST difference between the urban and rural areas is not significant at night. It indicates that the impact of the North Pacific Ocean on the nighttime UHI intensity in Vancouver is minimal.

In Toronto, the daytime LST in the urban area decreases as the distance to Lake Ontario gets closer, but beyond 4 kilometers, the daytime LST in the urban area does not change with distance (Figure 11). However, in the rural areas of Toronto within 2 kilometers from the water body, the daytime LST is lower when closer to the water body, and beyond 2 kilometers, the daytime LST decreases as the distance from the water body increases. Therefore, although Lake Ontario has little impact on the daytime LST in Toronto's urban area, it still influences the daytime LST in the rural areas to some extent, indicating that Lake Ontario has an effect on the daytime UHI intensity in Toronto. Furthermore, at night, although the variation trend of the LST in urban area is smooth, the LST in rural areas decreases significantly as the distance from the water body increases, leading to the increase of the LST diffe-

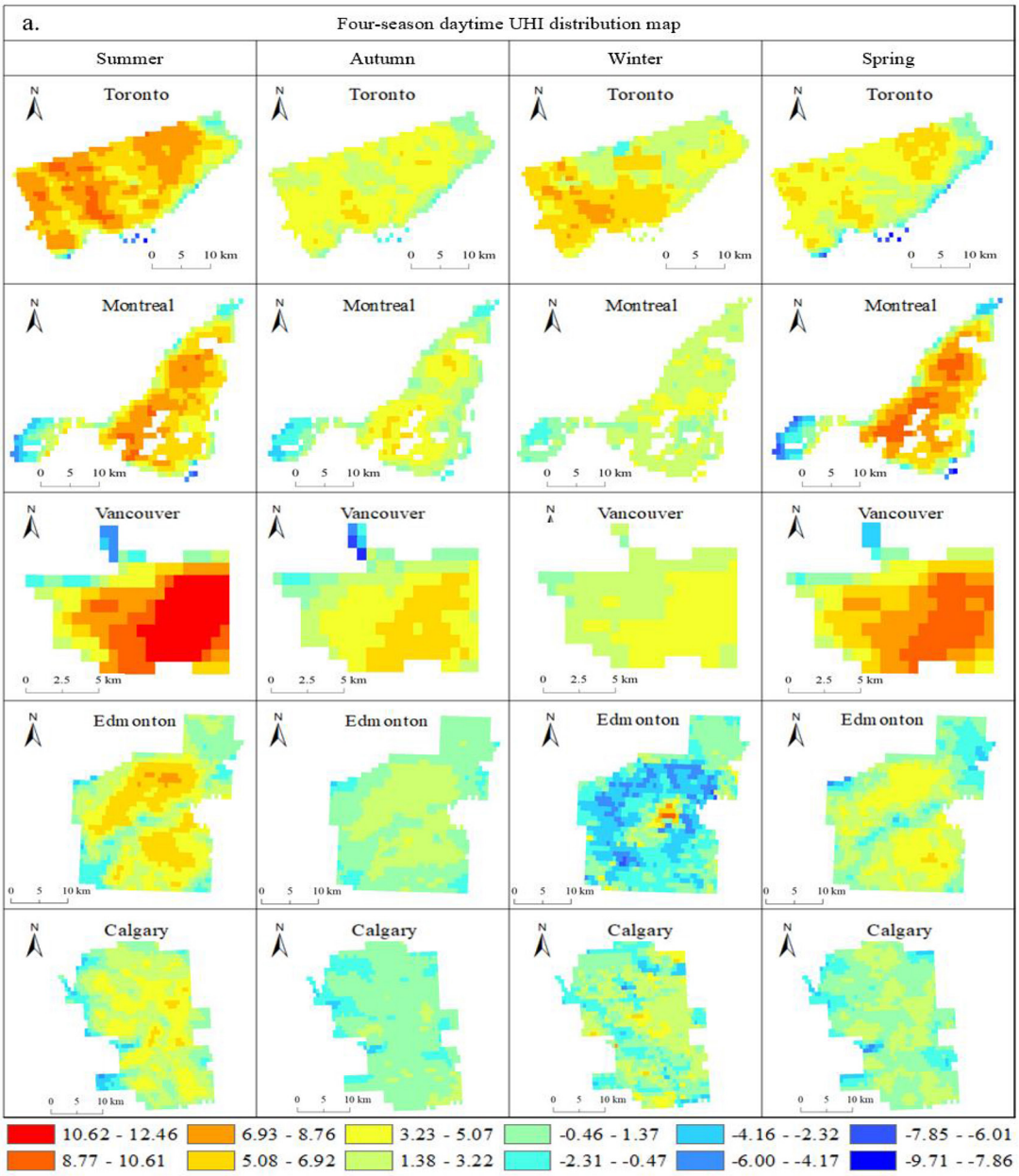

Figure 12a
Four-season daytime UHI intensity distribution maps across the cities

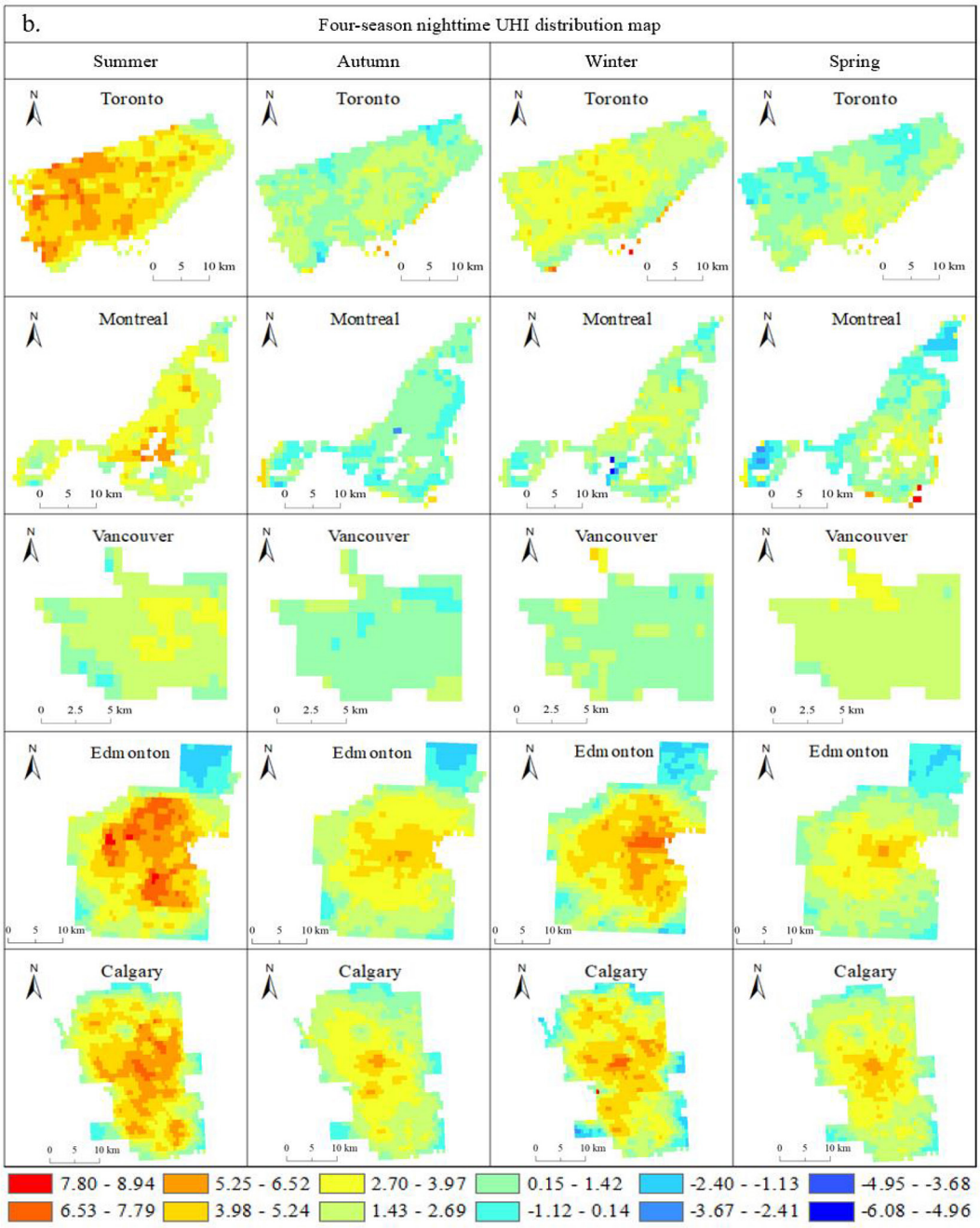

Figure 12b
Four-season nighttime UHI intensity distribution maps across the cities

rence. Therefore, Lake Ontario also has an effect on the nighttime UHI intensity in Toronto. In addition, although larger water bodies are closer to the urban area in both cities, we can still observe that they have a greater impact on rural areas than on urban areas.

Seasonal influence on day and night UHI intensity

As shown in Figures 12 and 13, the daytime and nighttime UHI intensity in all cities show obvious seasonal variation due to climatic influences and vegetation cover changes. The results indicate certain spatial differences in the UHI intensity across the four seasons. Notably, Edmonton and Calgary exhibit the most significant seasonal variations in UHI intensity. During the summer, autumn, and spring, their UHI intensity distribution trends are similar, but in the winter, they display contrasting patterns of UHI intensity distribution. Specifically, areas with higher UHI intensity in the summer, autumn, and spring become lower UHI intensity areas throughout the cities in the winter, particularly during daytime in Calgary and nighttime in Edmonton. On the other hand, Vancouver, Toronto, and Montreal exhibit consistent patterns of UHI distribution across all four seasons, although they experience lower UHI intensity values for the entire city during winter.

During the day, the highest peak summer UHI intensity value is found in Vancouver, reaching up to 12.46°C, while a region near Lake Ontario in Toronto has the lowest peak value at -8.30°C (Figure 12a). Obviously, in summer all five cities experience remarkably high daytime UHI intensity values encompassing their entire urban areas. In the autumn, the daytime UHI intensity starts to decline in all cities, and the regions showing relatively high UHI intensity values experience a substantial reduction in each city. However, the highest daytime UHI intensity values exceeded 3°C in all cities in autumn. Results show that both the highest and the lowest peak values in autumn are in Vancouver 6.39°C and at -4.82°C, respectively. During the winter months, the daytime UHI intensity values are lowest compared to other seasons. However, Vancouver is warmer than other cities in winter and shows a unique pattern with a greater than 0°C daytime UHI intensity across the entire city.

Calgary and Edmonton experience higher maximum daytime UHI intensity during the winter months compared to all other seasons. However, the central regions of Calgary and some urban areas of Edmonton display significant urban heat sinks (Figure 12a). In the spring, the daytime UHI intensity starts to increase in all the cities. Similar to summer, the highest daytime UHI intensity peak value is found in Montreal, reaching 10.42°C, while the lowest peak value is still observed along the lake in Toronto at -9.70°C. During the day, only Edmonton exhibits significant seasonal differences in UHI intensity distribution patterns, with an urban heat sink occurring in winter that differs from the other three seasons. In contrast, the other cities show roughly the same UHI intensity spatial patterns across all four seasons.

During the nighttime, all cities except Vancouver have a maximum summer UHI intensity value of 6.5°C or higher (Figure 12b). Edmonton reaches its peak summer UHI intensity value of 8.20°C, while Toronto and Calgary also experience a peak summer UHI intensity value of over 7.3°C. Moreover, in Edmonton, regions near the surrounding rural areas still maintain a lower nighttime UHI intensity value of -1.89°C in the summer. In the autumn, the peaks of the nighttime UHI intensity are substantially decreased in all cities. In Vancouver, the highest recorded autumn nighttime UHI intensity value is only 2.59°C, which is almost half of the peaks of the other four cities. Meanwhile, in Montreal, regions near the water surfaces have the lowest nighttime UHI intensity in the autumn, at -2.58°. During the winter season, Calgary and Edmonton show significant nighttime UHI intensity and the central parts of cities exhibit higher nighttime UHI intensity values. Besides, the highest peak winter nighttime UHI intensity value among the five cities is observed in Montreal, at 8.94°C and the lowest peak nighttime UHI intensity value is observed in Calgary, at -2.68°C. During winter, the nighttime UHI intensity in Vancouver remains above -0.01°C across the entire urban area. During the spring season, the nighttime UHI intensity significantly increased in Calgary, where the highest values reached 6.25°C from -1.08°C. However, the distribution patterns of spring nighttime UHI intensity in all five cities remain consistent with the rest of the seasons. At night, Edmonton and Calgary have similar UHI intensity spatial distribution patterns across all seasons, while Vancouver, Toronto, and Montreal show clear seasonal variations in their UHI spatial patterns.

During the daytime, all cities exhibit significant seasonal variations in the average four-season UHI intensity (Figure 13). For instance, Edmonton's average daytime UHI intensity value reach below -1°C during the winter months. Edmonton, Vancouver, and Montreal all have the lowest average daytime UHI intensity in winter, while Calgary and Toronto have the lowest daytime UHI intensity in autumn (Figure 13). Other than Montreal, where the highest daytime UHI intensity occurs in spring, all cities experience their highest daytime UHI intensity during

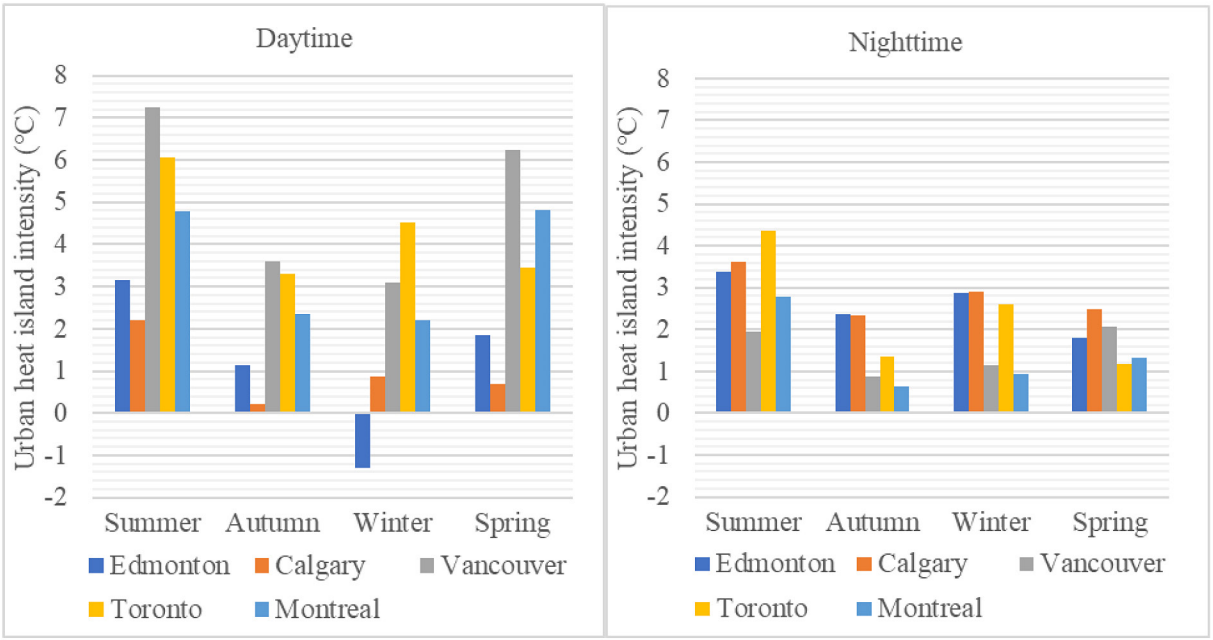

Figure 13
Four-season daytime and nighttime UHI intensity variation across the cities

the summer. Among all cities, Vancouver consistently records the highest daytime UHI intensity during summer, autumn, and spring, with values exceeding 3°C and even reaching over 7°C in summer. Toronto has the highest daytime UHI intensity only in winter, with a value exceeding 4°C. In general, the daytime UHI intensity of all the cities, except for Toronto, show similar patterns during the summer and spring, as well as during the autumn and winter. However, there is a significant difference between the warmer months (summer and spring) and the cooler months (autumn and winter).

In contrast, during the nighttime, the seasonal changes are smooth in all cities. In Edmonton, the nighttime UHI intensity remains above 1.5°C in all four seasons. Calgary exhibits the nighttime UHI intensity values above 2 °C for all seasons. In addition, the summer season exhibits the highest nighttime UHI intensity values as well. Vancouver, Calgary, and Montreal have the lowest nighttime UHI intensity in autumn, whereas Edmonton and Toronto have the lowest nighttime UHI intensity in spring. All five cities have average nighttime UHI intensity values greater than 1.6°. In addition, the nighttime UHI intensity values of Edmonton, Calgary and Toronto are above 3° during the summer months, making the UHI effect particularly significant during this period. Furthermore, Edmonton, Calgary and Toronto have higher nighttime UHI intensity values in winter compared to the autumn and spring, mainly attributable to lower LST and denser snow cover in rural areas compared to urban areas during the winter season.

Discussion

In this study, we conducted a comprehensive data collection and analysis of the daytime and nighttime LST for different land cover types in five Canadian cities, as well as their respective daytime and nighttime monthly UHI, seasonal UHI, and annual UHI distributions. The discussion section primarily focuses on exploring potential explanations for the findings.

Effect of geographic location and land cover type on daytime and nighttime LSTs

By comparing the daytime and nighttime LST of each city, we found that there are significant differences in the daytime and nighttime LST between cities. These differences are linked to the geography and the latitude of the cities, the city located at higher latitudes, like Edmonton which experiences longer cold periods, has lower annual

average land surface temperatures and the cities located at relatively mid latitudes, such as Vancouver and Toronto, have higher annual average land surface temperatures, which is consistent with the findings of Peng et al. (2012).

Additionally, different land use types also have varying impacts on LST. In most cities, built-up areas experience the highest daytime LST. This is because building materials absorb more solar radiation, causing the temperature to rise. However, in Vancouver, the grass area has the highest daytime LST. This may be due to the fact that most of the grass areas in Vancouver are scattered within built-up areas (Figure 3). As a result, the temperature of grass areas in downtown might be influenced by the surrounding built-up areas, leading to heat being trapped in the grass areas and causing higher daytime LST. Crop areas in cities such as Edmonton, Toronto, and Montreal have the lowest daytime LST, which is likely because in all three cities, the crop is distributed at the edge of the city, making their daytime LST lower than that of the city center areas. But in Vancouver, the treed area has the lowest daytime LST. In terms of Vancouver's geographic characteristics, trees near the ocean are affected by cold air, resulting in lower temperatures in these treed areas. As a result, the temperature difference in the treed areas is greater compared to the treed area in the downtown area, but surrounded by buildings. This observation aligns with the findings of Zhou et al. (2018) and Santamouris et al. (2017) on the UHI in the East China coastal region. In contrast, treed areas in Vancouver have the highest nighttime LST, which might be due to heat-trapping within the area (Coutts et al. 2016). Ultimately, through the analysis of LST for different land cover types, it is evident that the annual average daytime and nighttime LST in the built-up areas of each city corresponds closely with the overall situation of the annual average daytime and nighttime LST in each city described above. In this case, the LST in built-up area mainly influences the overall LST value, which is consistent with the findings of Chen et al. (2006) for the Pearl River Delta region of China.

In addition, the LST trends for different land cover types in cities are different between daytime and nighttime. Among all types of land cover, built-up areas have the most significant impact on daytime LST in almost all cities, while bare ground has the most significant impact on nighttime LST in Toronto and Montreal. Besides, large water bodies such as ocean or lake have a certain impact on the UHI in the waterfront areas of Vancouver and Toronto. At night, these large water bodies remain warmer than rural areas, continuing to warm the rural areas while their impact on urban areas diminishes, leading to an increase in nighttime UHI intensity. This explains the observed differences in UHI intensity distribution patterns between daytime and nighttime.

Variations in daytime and nighttime UHI across cities

Due to their varying geographic locations and climate conditions, the UHI effect differs among the five cities. For example, the urban heat sink phenomenon is observed in more areas of Calgary, as indicated by the results of this study. In contrast, Toronto and Vancouver have stronger UHI intensity during the day. Based on the study of Finnish cities, Drebs et al. (2023) also found that UHI intensity varies notably between cities and seasons in high-latitude regions, with urban structure, water bodies, and topography playing key roles. This is due to the fact that Calgary is located inland with an arid climate, while Toronto is situated in the Great Lakes region and Vancouver is by the coast, resulting in more humid climates for them. In humid regions, rural areas dissipate heat well due to high vegetation and precipitation, resulting in lower temperatures than urban areas, however, arid urban areas have stronger convective efficiency than rural ones, leading to lower urban temperatures and a negative heat island effect (Zhao et al., 2014). In arid cities, urban areas sometimes have higher soil moisture and vegetation cover than the surrounding rural areas. This can make cities cooler than the countryside, leading to an urban heat sink effect. Therefore, the daytime UHI intensity in the cities of arid inland areas is lower.

The study also found that each city exhibits a distinct difference in UHI between day and night. This is due to the different causes of daytime and nighttime UHI. During the day, the UHI effect is mainly due to the absorption and storage of solar radiation by building materials, while at night, the UHI effect is primarily caused by the release of the heat absorbed during the day (Oke, 1982; Oke, 1988). This leads to distinct variations in UHI phenomena between daytime and nighttime. During the day, Vancouver, Toronto, and Montreal experience higher UHI values, while at night, Calgary and Edmonton have higher UHIs compared to the other cities. These differences can be explained using the energy balance. The surface energy balance is described as:

$$Q + Q_A = E + H + G \quad \text{(Equation 6)}$$

where, Q is net radiation; Q_A is anthropogenic heat emissions; E is latent heat flux; H is sensible heat flux; G is ground heat flux (Clinton and Gong 2013; Friedl 2002; Price 1985; Rizwan et al. 2008; Taha 1997). The daytime UHI intensity is widely considered to be the result of a decrease in latent heat flux and an increase in sensible heat flux in urban areas due to a decrease in vegetation surfaces and an increase in impermeable surfaces (Voogt and Oke 2003). In other words, due to the changes in the amount of incident solar radiation, determined by the daytime length and sun angle, significant seasonal differences exist. For example, in summer, strong solar radiation with longer daylight causes higher temperatures in urban areas, while the increased transpiration from vegetation leads to lower temperatures in rural areas (Peng et al. 2012). This results in a higher UHI intensity during the daytime in summer. In addition, the research of Zhao et al. (2014), who studied the daytime UHI in various regions of North America under different climatic conditions, found that the daytime urban-rural temperature difference is also influenced by two factors: convective efficiency, which is related to aerodynamic forces and drag, as well as air humidity. They argued that in humid climate zones, heat dissipation through convection is lower in urban areas than in rural areas, thereby increasing the temperature in urban areas and resulting in the heat island effect (Zhao et al. 2014). In this regard, this could explain the high UHI intensity in Vancouver, even in the winter season that experiences high humidity levels.

At night, the heat flux to the air generally comes from radiative transfer, i.e. the thermal release of heat stored in urban areas during the day as well as the increase of anthropogenic heat emissions during the night (Masson 2000; Rizwan et al. 2008; Clinton and Gong 2013). During the day, building materials absorb thermal radiation and store heat. At night, buildings release this stored heat into the atmosphere, contributing to the nighttime UHI intensity (Oke 1982; 1988). Therefore, the nighttime UHI intensity is mainly determined by the size of the urban areas and the built-up structures (Sobstyl et al. 2018). The heat released at night usually enters and tends to accumulate in the lower atmosphere. As the air passes through urban areas, it accumulates more heat if it is further from the city's edge than to the city's center (Soltan and Sharifi 2017). This also explains why the UHI fluctuations in Vancouver are the smoothest. The small city size of Vancouver may also be responsible for the smoother UHI fluctuations, further affected by the surrounding ocean in moderating temperatures. Li et al. (2017) found that larger cities tend to have higher UHI intensity. Our results align with these previous observations. For example, under similar climatic conditions, altitudes, and geographic locations, Toronto and its surrounding built-up area cover approximately 1,570 square kilometers while Montreal and its surrounding built-up area cover around 966 square kilometers. As a result, Toronto experiences a higher UHI intensity compared to Montreal, as illustrated in Figure 6.

Li et al. (2017) also found that urban size in northern regions has a greater impact on UHI intensity compared to southern regions in the United States. Our study's results are consistent with these findings. This explains why Edmonton, Calgary, and Toronto experience higher UHI intensity at night. Moreover, during winter, the UHI intensity in Edmonton and Calgary is even higher than in Toronto, providing warmer benefits to the city in winter. However, some areas of Edmonton and Calgary show significant urban heat sinks in the winter. This might be attributed to the climate and related air pollution. Both cities experience harsh winters. At the same time, much of the power supplied to these cities are generated by coal- or natural gas-fired power plants, which leads to increased emissions of air pollutants. The aerosols masking, higher snow cover and lower building density, can reduce the amount of solar radiation reaching the ground and thereby reducing the absorption by urban surfaces (Zhou et al. 2015). Additionally, both Edmonton and Calgary are located in arid regions, where the vegetation cover and soil moisture within the urban areas are higher than in the surrounding rural areas, leading to lower temperatures in the urban areas. Consequently, a combination of air pollutants from human activities and the higher vegetation coverage within urban areas, influenced by climate conditions, leads to the urban heat sink during winter (Zhou et al. 2015).

Additionally, daytime UHI intensity is also influenced by the extent of land use changes that occur during urbanization (Zhou and Chen 2018). Urbanization has transformed most of the natural or semi-natural vegetative covers to impervious surfaces. Vegetation conducts transpiration during the day providing a cooling effect, particularly in rural areas. In contrast, impervious surfaces absorb the solar radiation, leading to higher daytime temperatures in urban areas. This creates a large daytime temperature difference between urban and rural areas. However, the vegetation cover has a smaller effect on nighttime UHI intensity, because vegetation does not conduct transpiration at night. In addition, the elevation differences between urban and rural areas, topographic features of the city and surrounding

areas, and the type of land use in the surrounding areas of the city all have an impact on the UHI as we observed in our results (Tang et al. 2022; Chen et al. 2017; Sun et al. 2019; Badaro-Saliba et al. 2021).

In addition, by studying the impact of large water bodies, i.e. the ocean, on the UHI in Vancouver, we found that the ocean has a significant positive effect on daytime UHI but a smaller impact on nighttime UHI. The research conducted by Miles et al. (2023) on seven Arctic cities in northern Europe showed that major coastal cities experience comparable daily variations in the UHI effect, supporting our results. According to the research conducted on cities in the Caspian Sea Plain, Firozjaei et al. (2023) demonstrated that during the day, ocean temperatures are lower than land temperatures, resulting in sea breezes cooling the surrounding air and lowering the UHI near the coast. Conversely, at night, ocean temperatures are higher than land temperatures, causing sea breezes to raise the temperatures in nearby areas and increase the UHI intensity near the coast. Similarly, our study indicates that the ocean has a cooling effect on urban areas during the day because their temperatures are lower than those of the surrounding urban areas, but higher than those of rural areas, thereby reducing the daytime UHI intensity.

Conclusions

Using remote sensing data from 2021, we studied the regional, seasonal and diurnal LST and UHI intensity variations in five major Canadian cities, and examined the effect of land cover types on the spatial distribution of LST across the cities. The average city UHI intensity values show higher daytime UHI intensity in all the city's central urban areas and a decrease towards the edges of cities or near water bodies. At night, , the UHI intensity is higher in the water bodies themselves and in built-up areas compared to other areas. Additionally, the study found that Vancouver, Toronto, and Montreal experience significantly higher daytime UHI effects across all four seasons compared to the cities of Edmonton and Calgary in the Prairies. However, during the nighttime, Edmonton and Calgary have higher UHI intensity than the other three cities. In all cities, daytime UHI exhibits significant seasonal variations, with the strongest UHI intensity in summer. In all five cities, both average daytime and nighttime UHI intensity showed significant variations across the year. Additionally, there are pronounced differences between day and night UHI values within these cities.

Geographic, latitude, and climate differences among the five Canadian cities result in distinct UHI distribution patterns, day-night changes, and seasonal variations, despite some commonalities. Edmonton and Calgary, influenced by higher latitudes and arid inland climates, experience lower daytime but higher nighttime UHI values with significant seasonal variability. Reducing building density and increasing tree cover can effectively mitigate UHI effects in these cities. Toronto and Vancouver, shaped by large water bodies and humid climates, have higher daytime and lower nighttime UHI values, with grass areas contributing to daytime LST. Strategies such as reducing building density, developing built-up areas trapped in heat, and replacing grass with trees can help. Additionally, Toronto's large size and higher built area exacerbate UHI effects, which could be mitigated by developing more green canopies and green roofs for large buildings. Montreal, with its mid-latitude, modest elevation, and smaller size, shows less pronounced UHI patterns. Planting trees on bare lands and reducing building density could alleviate UHI in Montreal.

Moreover, policymakers can leverage the similarities in UHI distribution patterns to exchange insights and use the observed differences between cities as a basis to develop or adapt UHI mitigation strategies based on the local circumstances. For instance, Edmonton and Calgary could exchange insights to improve their UHI mitigation strategies, while Vancouver and Toronto could benefit from each other's experiences due to their proximity to large water bodies. Montreal, with its humid climate, might adopt policies similar to those of Vancouver and Toronto, but should also create tailored strategies that address its smaller urban and built-up areas. Furthermore, since these five cities are highly representative, other Canadian cities could use the UHI characteristics identified in this analysis to enhance their own UHI mitigation policies. Incorporating UHI effects into high-latitude urban and regional planning can offer significant benefits for both summer and winter conditions. By implementing strategies to mitigate UHI, such as increasing urban vegetation, installing green roofs, and using reflective materials, cities can effectively reduce the heat generated in urban areas during the summer, which lowers energy consumption and enhances comfort. In Edmonton, Calgary and Montreal, the expansion of vegetated areas, particularly through the planting of diverse tree and shrub species, demonstrated a notable cooling effect on UHI intensity, whereas grass cover alone contributed minimally to temperature reduction. In addition, in Vancouver and Toronto, the presence and enhancement of urban water bodies also played a significant role in mitigating surface UHI. Managing UHI can provide winter benefits such as reduced energy demands for heating and fewer cold-related deaths during cooler months. This approach

helps prevent extreme temperature fluctuations, potentially reducing heating costs during the winter. Thus, this study also provides valuable insights for analyzing urban climate change. Future research could be conducted using advanced technologies, such as machine learning, to analyze a broader range of cities and achieve more comprehensive results. Additionally, future research could incorporate anthropogenic heat emissions from transportation, industrial activities, and energy consumption to provide a more comprehensive assessment of UHI dynamics. Further, integrating urban morphological characteristics, such as sky view factor, street canyon effects, and the thermal properties of built surfaces (e.g., surface albedo and emissivity), could enhance the understanding of how urban form influences heat retention and distribution. By considering these factors, future studies can improve the accuracy of UHI analyses and contribute to more effective urban climate adaptation strategies.

Limitations and future study

This study focused on the seasonal and diurnal variation of UHI intensity across five Canadian cities, emphasizing the differences between cities and the influence of land use types. However, several limitations should be noted. First, the study did not examine finer-scale urban characteristics such as city size, building density, and urban spatial layout, which are known to significantly affect UHI formation. Second, microscale urban features, including street canyon geometry, building height, and the spatial distribution of green spaces, were not incorporated due to data limitations and the broader spatial focus of this research. Third, anthropogenic influences such as energy consumption, traffic emissions, and industrial activities were not quantitatively analyzed, which may limit the understanding of UHI drivers. Future research should incorporate high-resolution urban form metrics, surface thermal properties, and human activity data. Advanced methods such as machine learning may also help extend the analysis to more cities and long-term dynamics and improve spatial accuracy. Addressing these aspects will enhance UHI modeling and support more effective urban heat mitigation strategies.

Acknowledgements

We acknowledge the use of Google Earth Engine to conduct this research.

Data availability

Data will be made available on request.

References

Acosta, M. P., M. Dikkers, F. Vahdatikhaki, J. Santos, and A. G. Dorée. 2023. A comprehensive generalizability assessment of data-driven Urban Heat Island (UHI) models. *Sustainable Cities and Society* 96: 104701. https://doi.org/10.1016/j.scs.2023.104701.

Assaf, G., and R. H. Assaad. 2023. Models and methods for quantifying the benefits of engineered heat mitigation initiatives: A critical review. *Urban Climate* 51: 101654. https://doi.org/10.1016/j.uclim.2023.101654.

Badaro-Saliba, N., J. Adjizian-Gerard, R. Zaarour, and G. Najjar. 2021. LCZ scheme for assessing Urban Heat Island intensity in a complex urban area (Beirut, Lebanon). *Urban Climate* 37: 100846. https://doi.org/10.1016/j.uclim.2021.100846.

BC Coroners Service. 2022. *Extreme heat and human mortality: A review of heat-related deaths in BC in summer 2021*.

Chen, X. L., H. M. Zhao, P. X. Li, Z. Y. Yin. 2006. Remote sensing image-based analysis of the relationship between urban heat island and land use/cover changes. *Remote Sensing of Environment* 104(2)L 133–146. https://doi.org/10.1016/j.rse.2005.11.016.

Chen, Y. C., H. W. Chiu, Y. F. Su, Y. C. Wu, and K. S. Cheng. 2017. Does urbanization increase diurnal land surface temperature variation? Evidence and implications. *Landscape and Urban Planning* 157: 247–258. https://doi.org/10.1016/j.landurbplan.2016.06.014.

Chien, F., C. C. Hsu, L. Ozturk, A. Sharif, and M. Sadiq. 2022. The role of renewable energy and urbanization towards greenhouse gas emission in top Asian countries: Evidence from advance panel estimations. *Renewable Energy* 186: 207–216. https://doi.org/10.1016/j.renene.2021.12.118.

Clinton, N., and P. Gong. 2013. MODIS detected surface urban heat islands and sinks: Global locations and controls. *Remote Sensing of Environment* 134, 294–304. https://doi.org/10.1016/j.rse.2013.03.008.

Coutts, A. M., E. C. White, N. J. Tapper, J. Beringer, and S. J. Livesley. 2016. Temperature and human thermal comfort effects of street trees across three contrasting street canyon environments. *Theoretical and Applied Climatology* 124: 55-68. https://doi.org/10.1007/s00704-015-1409-y.

Dalby, S. 2002. Security and ecology in the Age of Globalization. *Environmental Change and Security Project Report*, 8(101): 4.

Drebs, A., J. Suomi, and A. Mäkelä. 2023. Urban heat island research at high latitudes—utilising Finland as an example. *Boreal Environment Research* 28, 81–96.

Esri, Microsoft. 2022. Sentinel-2 10m Land Use/Land Cover Timeseries Downloader. [data set]. Sentinel-2 10m Land Use/Land Cover Timeseries Downloader (Mature Support) (arcgis.com).

Esri. (n.d.). *How High/Low Clustering (Getis-Ord General G) works—ArcGIS Pro*. https://pro.arcgis.com/en/pro-app/3.0/tool-reference/spatial-statistics/h-how-high-low-clustering-getis-ord-general-g-spat.htm.

Firozjaei, M. K., A. Sedighi, N. Mijani, Y. Kazemi, and F. Amiraslani. 2023. Seasonal and daily effects of the sea on the surface urban heat island intensity: A case study of cities in the Caspian Sea Plain. *Urban Climate* 51: 101603. https://doi.org/10.1016/j.uclim.2023.101603.

Friedl, M. A. 2002. Forward and inverse modeling of land surface energy balance using surface temperature measurements. *Remote Sensing of Environment* 79(2–3): 344–354. https://doi.org/10.1016/S0034-4257(01)00284-X.

Gaur, A., M. K. Eichenbaum, and S. P. Simonovic. 2018. Analysis and modelling of surface Urban Heat Island in 20 Canadian cities under climate and land-cover change. *Journal of Environmental Management* 206: 145–157. https://doi.org/10.1016/j.jenvman.2017.10.002.

Hardin, A. W., Y. Liu, G. Cao, J. K. Vanos. 2018. Urban heat island intensity and spatial variability by synoptic weather type in the northeast US. *Urban Climate* 24: 747–762. https://doi.org/10.1016/j.uclim.2017.09.001.

Hayes, A. T., Z. Jandaghian, M. A. Lacasse, A. Gaur, H. Lu, A. Laouadi, A., H. Ge, and L. Wang. 2022. Nature-based solutions (nbss) to mitigate urban heat island (UHI) effects in Canadian cities. *Buildings* 12(7): 925. https://doi.org/10.3390/buildings12070925.

Health Canada. 2020. *Reducing urban heat islands to protect health in Canada*. https://www.canada.ca/en/services/health/publications/healthy-living/reducing-urban-heat-islands-protect-health-canada.html.

Hoornweg, D., L. Sugar, and C. L. Trejos Gómez. 2011. Cities and greenhouse gas emissions: Moving forward. *Environment and Urbanization* 23(1): 207–227. https://doi.org/10.1177/0956247810392270.

Imhoff, M. L., P. Zhang, R. E. Wolfe, and L. Bounoua. 2010. Remote sensing of the urban heat island effect across biomes in the continental USA. *Remote Sensing of Environment* 114(3): 504–513. https://doi.org/10.1016/j.rse.2009.10.008.

Kornhuber, K., S. Osprey, D. Coumou, S. Petri, V. Petoukhov, S. Rahmstorf, and L. Gray. 2019. Extreme weather events in early summer 2018 connected by a recurrent hemispheric wave-7 pattern. *Environmental Research Letters* 14(5): 054002. DOI 10.1088/1748-9326/ab13bf.

Li, X., and W. Zhou. 2019. Spatial patterns and driving factors of surface urban heat island intensity: A comparative study for two agriculture-dominated regions in China and the USA. *Sustainable Cities and Society* 48: 101518. https://doi.org/10.1016/j.scs.2019.101518.

Li, X., Y. Zhou, G. R. Asrar, M. Imhoff, and X. Li. 2017. The surface urban heat island response to urban expansion: A panel analysis for the conterminous United States. *Science of the Total Environment* 605: 426–435. https://doi.org/10.1016/j.scitotenv.2017.06.229.

Lowe, S. A. 2016. An energy and mortality impact assessment of the urban heat island in the US. *Environmental Impact Assessment Review* 56: 139–144. https://doi.org/10.1016/j.envint.2021.106530.

Macintyre, H. L., C. Heaviside, X. Cai, and R. Phalkey. 2021. The winter urban heat island: Impacts on cold-related mortality in a highly urbanized European region for present and future climate. *Environment International* 154: 106530. https://doi.org/10.1016/j.envint.2021.106530.

Maimaitiyiming, M., A. Ghulam, T. Tiyip, F. Pla, P. Latorre-Carmona, Ü. Halik, Ü., M. Sawut, and M. Caetano. 2014. Effects of green space spatial pattern on land surface temperature: Implications for sustainable urban planning and climate change adaptation. *ISPRS Journal of Photogrammetry and Remote Sensing* 89: 59–66. https://doi.org/10.1016/j.isprsjprs.2013.12.010.

Manley, G. 1958. On the frequency of snowfall in metropolitan England. *Quarterly Journal of the Royal Meteorological Society* 84(359): 70–72. https://doi.org/10.1002/qj.49708435910.

Masson, V. 2000. A physically-based scheme for the urban energy budget in atmospheric models. *Boundary-layer Meteorology* 94: 357–397. https://doi.org/10.1023/A:1002463829265.

Miles, V., and I. Esau. 2017. Seasonal and spatial characteristics of urban heat islands (UHIs) in northern West Siberian cities. *Remote Sensing* 9(10): 989. https://doi.org/10.3390/rs9100989.

Miles, V., and I. Esau. 2020. Surface urban heat islands in 57 cities across different climates in northern Fennoscandia. *Urban Climate* 31: 100575. https://doi.org/10.1016/j.uclim.2019.100575.

Miles, V., I. Esau, and M. W. Miles. 2023. The urban climate of the largest cities of the European Arctic. *Urban Climate* 48: 101423. https://doi.org/10.1016/j.uclim.2023.101423.

Newbold, K. B. 2011. Urbanisation and the growth of the Canadian city. *The changing Canadian population*. Berlin, DE: De Gruyter Brill, 175–188.

NOAA. 2021. *Global climate report – December 2021*. National Centers for Environmental Information. https://www.ncei.noaa.gov/news/global-climate-202112.

Oke, T. R. 1973. City size and the urban heat island. *Atmospheric Environment* 1967 7(8): 769–779. https://doi.org/10.1016/0004-6981(73)90140-6.

——. 1982. The energetic basis of the urban heat island. *Quarterly Journal of the Royal Meteorological Society* 108(455): 1–24. https://doi.org/10.1002/qj.49710845502.

——. 1988. Street design and urban canopy layer climate. *Energy and Buildings* 11(1–3): 103–113. https://doi.org/10.1016/0378-7788(88)90026-6.

Parker, D. E. 2010. Urban heat island effects on estimates of observed climate change. *Wiley Interdisciplinary Reviews: Climate Change* 1(1): 123–133. https://doi.org/10.1002/wcc.21.

Peng, S., S. Piao, P. Ciais, P. Friedlingstein, C. Ottle, F. M. Bréon, H. Nan, and R. B. Myneni. 2012. Surface urban heat island across 419 global big cities. *Environmental Science & Technology* 46(2): 696–703. https://doi.org/10.1021/es2030438.

Price, J. C. 1985. On the analysis of thermal infrared imagery: The limited utility of apparent thermal inertia. *Remote sensing of Environment* 18(1): 59–73. https://doi.org/10.1016/0034-4257(85)90038-0.

Rinner, C., amd M. Hussain. 2011. Toronto's urban heat island—Exploring the relationship between land use and surface temperature. *Remote Sensing* 3(6): 1251–1265. https://doi.org/10.3390/rs3061251.

Rizwan, A. M., L. Y. Dennis, and L. I. U. Chunho. 2008. A review on the generation, determination and mitigation of Urban Heat Island. *Journal of Environmental Sciences* 20(1): 120–128. https://doi.org/10.1016/S1001-0742(08)60019-4.

Santamouris, M. 2015. Analyzing the heat island magnitude and characteristics in one hundred Asian and Australian cities and regions. *Science of the Total Environment* 512: 582–598. https://doi.org/10.1016/j.scitotenv.2015.01.060.

Santamouris, M., S. Haddad, F. Fiorito, P. Osmond, L. Ding, D. Prasad, D., X. Zhai, and R. Wang. 2017. Urban heat island and overheating characteristics in Sydney, Australia. An analysis of multiyear measurements. *Sustainability* 9(5): 712. https://doi.org/10.3390/su9050712.

Schneider, A., M. A. Friedl, and D. Potere. 2009. A new map of global urban extent from MODIS satellite data. *Environmental Research Letters* 4(4): 044003.

Schwarz, N., U. Schlink, U. Franck, and K. Großmann. 2012. Relationship of land surface and air temperatures and its implications for quantifying urban heat island indicators—An application for the city of Leipzig (Germany). *Ecological Indicators* 18: 693–704. https://doi.org/10.1016/j.ecolind.2012.01.001.

Sidiqui, P., A. Huete, and R. Devadas. 2016, July. Spatio-temporal mapping and monitoring of urban heat island patterns over Sydney, Australia using MODIS and Landsat-8. In 2016 4th International Workshop on Earth Observation and Remote Sensing Applications (EORSA), 217–221. IEEE. doi: 10.1109/EORSA.2016.7552800.

Sobstyl, J. M., T. Emig, M. A. Qomi, F. J. Ulm, and R. M. Pellenq. 2018. Role of city texture in urban heat islands at nighttime. *Physical Review Letters* 120(10): 108701. https://doi.org/10.1103/PhysRevLett.120.108701.

Soltani, A., and E. Sharifi. 2017. Daily variation of urban heat island effect and its correlations to urban greenery: A case study of Adelaide. *Frontiers of Architectural Research* 6(4): 529–538. https://doi.org/10.1016/j.foar.2017.08.001.

Statistics Canada. 2022. *Census profile, 2021 census of population*. https://www12.statcan.gc.ca/census-recensement/2021/dp-pd/prof/index.cfm?Lang=E.

Stewart, I. D. 2011. A systematic review and scientific critique of methodology in modern urban heat island literature. *International Journal of Climatology* 31(2): 200–217. https://doi.org/10.1002/joc.2141.

Sun, Y., C. Gao, J. Li, R. Wang, and J. Liu. 2019. Evaluating urban heat island intensity and its associated determinants of towns and cities continuum in the Yangtze River Delta Urban Agglomerations. *Sustainable Cities and Society* 50: 101659. https://doi.org/10.1016/j.scs.2019.101659.

Taha, H. 1997. Urban climates and heat islands: Albedo, evapotranspiration, and anthropogenic heat. *Energy and Buildings* 25(2): 99–103. https://doi.org/10.1016/S0378-7788(96)00999-1.

Tang, J., X. Lan, Y. Lian, F. Zhao, and T. Li. 2022. Estimation of urban–rural land surface temperature difference at different elevations in the Qinling–Daba Mountains using MODIS and the Random Forest Model. *International Journal of Environmental Research and Public Health* 19(18): 11442. https://doi.org/10.3390/ijerph191811442.

Tomlinson, C. J., L. Chapman, J. E. Thornes, and C. J. Baker. 2012. Derivation of Birmingham's summer surface urban heat island from MODIS satellite images. *International Journal of Climatology* 32(2): 214–224. https://doi.org/10.1002/joc.2261.

Voogt, J. A., and T. R. Oke. 2003. Thermal remote sensing of urban climates. Remote Rensing of Environment, 86(3): 370–384. https://doi.org/10.1016/S0034-4257(03)00079-8.

Wan, Z. 2014. New refinements and validation of the collection-6 MODIS land-surface temperature/emissivity product. *Remote Sensing of Environment* 140: 36–45. https://doi.org/10.1016/j.rse.2013.08.027.

Wang, A., Y. Dai, M. Zhang, and E. Chen. 2025. Exploring the cooling intensity of green cover on urban heat island: A case study of nine main urban districts in Chongqing. *Sustainable Cities and Society* 124: 106299. https://doi.org/10.1016/j.scs.2025.106299.

Wang, Y., U. Berardi, and H. Akbari. 2016. Comparing the effects of urban heat island mitigation strategies for Toronto, Canada. *Energy and Buildings* 114: 2–19. https://doi.org/10.1016/j.enbuild.2015.06.046.

Welegedara, N. P., S. K. Agrawal, and G. Lotfi. 2023. Exploring spatiotemporal changes of the urban heat Island effect in high-latitude cities at a neighbourhood level: A case of Edmonton, Canada. *Sustainable Cities and Society* 90: 104403. https://doi.org/10.1016/j.scs.2023.104403.

Wienert, U., and W. Kuttler. 2005. The dependence of the urban heat island intensity on latitude-A statistical approach. *Meteorologische Zeitschrift* 14(5): 677–686. DOI: 10.1127/0941-2948/2005/0069.

Zhang, Y., D. Hu, S. Cao, S. Chen, and C. Yu. 2018. Remote sensing monitoring of heat island intensity in Beijing-Tianjin-Hebei urban agglomeration and analysis of urban scale effect. *Journal of Capital Normal University* (Natural Science Edition) 39(5): 72–80. DOI:10.19789/j.1004-9398.2018.05.015.

Zhao, L., X. Lee, R. B. Smith, and K. Oleson. 2014. Strong contributions of local background climate to urban heat islands. *Nature* 511(7508): 216–219. https://doi.org/10.1038/nature13462.

Zhou, D., S. Bonafoni, L. Zhang, and R. Wang. 2018. Remote sensing of the urban heat island effect in a highly populated urban agglomeration area in East China. *Science of the Total Environment* 628: 415–429. https://doi.org/10.1016/j.scitotenv.2018.02.074.

Zhou, D., S. Zhao, S. Liu, L. Zhang, and C. Zhu. 2014. Surface urban heat island in China's 32 major cities: Spatial patterns and drivers. *Remote Sensing of Environment* 152: 51–61. https://doi.org/10.1016/j.rse.2014.05.017.

Zhou, D., S. Zhao, L. Zhang, G. Sun, and Y. Liu. 2015. The footprint of urban heat island effect in China. *Scientific Reports* 5(1): 11160. https://doi.org/10.1038/srep11160.

Zhou, X., and H. Chen. 2018. Impact of urbanization-related land use land cover changes and urban morphology changes on the urban heat island phenomenon. *Science of the Total Environment* 635: 1467–1476. https://doi.org/10.1016/j.scitotenv.2018.04.091.

Zhu, W., A. Lű, and S. Jia. 2013. Estimation of daily maximum and minimum air temperature using MODIS land surface temperature products. *Remote Sensing of Environment* 130: 62–73. https://doi.org/10.1016/j.rse.2012.10.034.